

See discussions, stats, and author profiles for this publication at: <https://www.researchgate.net/publication/362410716>

Evaluating the efficiency of popular species identification analytical methods, and integrative workflow using morphometry and barcoding bioinformatics for taxonomy and origin of t...

Article in *Global Ecology and Conservation* · August 2022

DOI: 10.1016/j.gecco.2022.e02253

CITATIONS

0

9 authors, including:



Siti N. Othman
Nanjing Forestry University

23 PUBLICATIONS 48 CITATIONS

[SEE PROFILE](#)

READS

48



Yuchol Shin
Kangwon National University

32 PUBLICATIONS 49 CITATIONS

[SEE PROFILE](#)



Ming-Feng Chuang
National Chung Hsing University

28 PUBLICATIONS 132 CITATIONS

[SEE PROFILE](#)



Yoon Hyuk Bae
Nanjing Forestry University

36 PUBLICATIONS 136 CITATIONS

[SEE PROFILE](#)

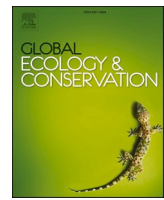
Some of the authors of this publication are also working on these related projects:



2020 Call for Papers - Special Issue: "Impact of Anthropogenic Activities on Amphibians and Reptiles: Threats and Conservation" [View project](#)



Diversity, Distribution and Ecology of Herpetofauna of Eastern India [View project](#)



Evaluating the efficiency of popular species identification analytical methods, and integrative workflow using morphometry and barcoding bioinformatics for taxonomy and origin of traded cryptic brown frogs

Siti N. Othman ^{a,b}, Yucheol Shin ^{a,c}, Hyun-Tae Kim ^d, Ming-Feng Chuang ^e,
Yoonhyuk Bae ^{a,b}, Jennifer Hoti ^{b,f}, Yong Zhang ^g, Yikweon Jang ^{b,*}, Amaël Borzée ^{a,*}

^a Laboratory of Animal Behaviour and Conservation, College of Biology and the Environment, Nanjing Forestry University, 159 Longpan Rd, Nanjing, Jiangsu, China

^b Department of Life Sciences and Division of EcoScience, Ewha Womans University 03760, Republic of Korea

^c Department of Biological Sciences, College of Natural Science, Kangwon National University, Chuncheon 24341, Republic of Korea

^d Seosan Joongang High School, Seosan 32027, Republic of Korea

^e Department of Life Sciences and Research Center for Global Change Biology, National Chung Hsing University, Taichung 402, Taiwan

^f Department of Life Sciences and Systems Biology, University of Turin, Turin, Italy

^g Co-Innovation Center for Sustainable Forestry in Southern China, College of Biology and the Environment, Nanjing Forestry University, Nanjing 210037, China

ARTICLE INFO

Keywords:

Agricultural trade
Northeast Asia
Rana
Species delimitation
Cryptic
Alien-invasive

ABSTRACT

The unregulated wildlife trade increases the risk of global biological invasions and, therefore, accurate taxonomic assignments and origin-tracing methods are critical. First, using a meta-analysis comparing studies from the last 10 years, we quantified the efficiency of popular analytical methods used for species assignments and confirmed the higher sensitivity of coalescent-based methods in isolating cryptic operational taxonomic units (OTUs). Second, we proposed a workflow for species identification of unidentified animals from the trade, in this case cryptic Brown frogs (*Rana*) imported into the Republic of Korea. This integrated workflow relies on the use of a single-locus 16S rRNA gene barcoding along with morphometry, phylogenetic trait, species delimitation modelling and phylogeography. Out of 171 samples, we identified three erroneously imported non-native species: *R. chensinensis*, *R. amurensis* and *R. kukunoris*. Bayes factor delimitation modelling most supported the presence of 12 OTUs from the trade, highlighting a hidden genetic diversity. Both molecular and morphological analyses converged towards a high phenotypic crypticity and similarity in genetic sequences between Korean *R. huanrenensis* and Chinese *R. chensinensis*. The combined model-based OTUs and 16S rRNA gene phylogeny of traded and control specimens ($n = 230$) recovered the trade pathways, and revealed the widespread and likely wild-harvested origins of traded *Rana* individuals. Our results also highlight the independent evolution of toe webbings in *Rana* for the last 12.0 Mya, a potential key trait for species identification of northeastern Asian *Rana*. With the workflow for large-scale

* Corresponding authors.

E-mail addresses: dy.othman@gmail.com (S.N. Othman), brongersmai2@gmail.com (Y. Shin), pintail1@naver.com (H.-T. Kim), adammfc@gmail.com (M.-F. Chuang), gyyh0303@gmail.com (Y. Bae), jennifer.hoti12@gmail.com (J. Hoti), Yong.zhang@njfu.edu.cn (Y. Zhang), jang@ewha.ac.kr (Y. Jang), amaelborzee@njfu.edu.cn (A. Borzée).

species identification developed herein, we urge the development of trade monitoring and legislation on *Rana* species in northeast Asia.

1. Introduction

Unsustainable wildlife trade results in the exploitations and loss of biodiversity (Morton et al., 2021), jeopardise the environments and ecosystems (Hughes et al., 2021), promote biological invasions and impact human health (Borzée et al., 2020a, 2020b). Specifically, biological invasions negatively impact the environment, and contribute to global biodiversity declines by outcompeting for resources with native communities (Sakai et al., 2001). Biological invasions also have to potential to exacerbate the transmission of zoonotic diseases to both wildlife (O'Hanlon et al., 2018) and humans (Borzée et al., 2021a). Contrary to the gradual impacts of environmental pressure, anthropogenic activities have accelerated the tempo of biological invasions (Pyšek et al., 2010). Most cases of biological invasions originate from the inadvertent introduction of species through human activities such as trading (Hulme, 2009). Biological invasions thus result primarily from human errors (Horvitz et al., 2017), and therefore make them preventable (Faulkner et al., 2020). However, the prevention of anthropogenic biological invasion is hindered by the inability to identify potential invasive species (Jarić et al., 2019), mostly due to crypticity in phenotypic variance (Morais and Reichard, 2018).

Biological invasions resulting from the wildlife trade have been reported worldwide, in increasingly high numbers and impact (Hughes et al., 2021): America (Schloegel et al., 2009), Europe (Auliya et al., 2016a, 2016b), Africa (Vandome and Vines, 2018), Oceania (García-Díaz et al., 2017) and Southeast Asia (Nijman and Shepherd, 2011). Particularly, the amphibian trade in East Asia has resulted in global biosecurity crisis: (1) the Korean peninsula is considered the ground zero for the amphibian chytrid fungus (*Batrachochytrium dendrobatidis*), the pathogen that caused the largest number of documented species extinctions worldwide (O'Hanlon et al., 2018); (2) eastern Asia is the origin of *B. salamandrivorans* (Laking et al., 2017), and the fungal pathogen reached Europe and likely North America through the international trade (Waddle et al., 2020); (3) Ranids are a vector for ranavirus (Schloegel et al., 2009), and the first cases of ranavirus were recently found in wild population of *Rana uenoi* in the Republic of Korea (Park et al., 2021).

Following decades of weak biosecurity regulations (Mun et al., 2013; Kil and Kim, 2014), wildlife trade policies in the Republic of Korea are slowly catching up with some of the threats linked to the trade (Borzée et al., 2020a). However, such recent improvements are still inadequate to detect potential breaches in the biosecurity regulations and potential bioinvasion events. In anurans, for example, there is lack of attention on potentially invasive species, with the exception of a once adequate but now abolished regulations for the American bullfrog, *Lithobates catesbeianus* (Groffen et al., 2019). However, even in the presence of adequate trade regulations, highly conserved morphological traits of traded species may hinder enforcement of such regulations. The large-scale introduction of the highly cryptic brown frogs through the amphibian trade into the country studied here provides a fresh input for the exploration of efficient species assignments tools to infer potential invasions. Due to the lack of morphological distinctiveness (Kim et al., 2002), wide divergence in genetics (Vences et al., 2013; Yuan et al., 2016) and their presence in the trade, the brown frogs, *Rana* sp. are a perfect model system to investigate cryptic biological invasion events and the establishment of key identification framework using phenotypic and genetic traits.

Effective species identification is an essential conservation tool to prevent early biological invasion, especially when the potential invaders are sourced from the wildlife trade (Marshall et al., 2020; Hughes et al., 2021). For instance, there are currently three species of Brown frogs in the genus *Rana* recognized in the Republic of Korea: *R. uenoi*, *R. coreana*, and *R. huanrenensis*. However, only native species that are also distributed outside the country can be legally imported, i.e. *R. huanrenensis*, and the identity of the *Rana* traded is largely unchecked and remains dubious due to the absence of an identification framework. In addition, surplus animals from the trade are regularly released into the wild at the end of each trading season. This situation therefore presents potential breaches in biosecurity and opportunities for cryptic invasions by non-native species. However, the current comparative approaches for species assignment, whether it is morphology- or DNA sequence-based, are limited by two issues: inaccuracy (Camargo et al., 2012; Reid and Carstens, 2012) and inconsistency (Taylor et al., 2017). For instance, meristic variations provide useful cues for morphology-based identification of known native *Rana* species. However, such meristic characters may not be useful to identify unknown species, as the characters have not been characterised for geographically distant congeneric species. Furthermore, no consistent information on morphological variables has been determined to identify all northeast Asian *Rana* through the sole use of morphology (refer to Table S1). Only large scale studies successfully manage to address the morphological convergence between clades, such as between *R. uenoi* and *R. dybowskii* (Yang et al., 2017), and molecular identification is the most reliable method for accurate species identification (Othman et al., 2020b). Thus, screening of *Rana* sp. through conventional neutral markers and barcoding is generally needed (Vences et al., 2013).

Barcodeing based on a single locus is sufficient, cost effective (Stouthamer and Nunney, 2014), and hence pertinent for the identification of most species (Yang et al., 2014) and evolutionary significant unit (ESU; Robertson et al., 2014). However, the use of neutral markers for barcodeing only can also be insufficient (Rubinoff and Holland, 2005), especially for hyper diverse group of species (Fourdrilis and Backeljau, 2019) because of mitonuclear discordance and introgression between closely related clades (Zhou et al., 2012). Thus, increasing the accuracy of single locus barcodeing is critical (Zhao et al., 2018). In addition, phylogeography is an essential tool to detect spatial crypticity and numerous studies on anuran invasions have relied on phylogeography to retrace invasion pathways (Mohanty and Measey, 2019; Othman et al., 2020a). Another alternative to overcome the shortcoming of barcodeing is the use of sequence similarity in operational taxonomical unit (OTU) phylogenies to increase the accuracy of clustering (Nguyen et al., 2016). Similarly, the implementation of model-based OTUs in phylogeography can help reconstruct the spatial native range of invasive

species.

Basic distance-based species delimitation method such as the Automatic Barcode Gap Discovery (ABGD; [Puillandre et al., 2012](#)) serves as primary tool to detect significant barcode gaps to partition the data. When needed, integrative taxonomic tools such as comparative species delimitations can also be used to tackle taxonomic conundrum ([Firkowski et al., 2016](#); [Correa et al., 2017](#); [Chan and Grismer, 2019](#)). However, this type of advances is rarely used for large-scale species assignments, as required for the control of wildlife trade, when the integration between species delimitation model and OTU-based phylogeography can be used to retrace the origins of traded specimens. Alternatively, Bayesian coalescent-based species delimitations can help resolve more complex taxonomic problems. It is an efficient tool to trace young diverging clades ([Birch et al., 2017](#)), although it can be influenced by geographical range ([Gaytán et al., 2020](#)) and isolation by distance ([Mason et al., 2020](#)). Species delimitation tools based on coalescence such as the Generalised Mixed Yule Coalescence Method (GMYC; [Fujisawa and Barraclough, 2013](#)) and the Bayesian implementation on Poisson Tree Processes (bPTP; [Zhang et al., 2013a](#)) are generally less conservative, with a tendency to predict more OTUs than morphometric analyses ([Talavera et al., 2013](#)), outperforming the conventional distance-based species delimitation ([Nguyen et al., 2016](#); [Yu et al., 2017](#)). Nevertheless, the lack of consistency in performance and conservatism of these species assignment methods across studies ([Fig. S1-S6](#)) highlights the need for comparisons on the efficacy of different methods in resolving taxonomy of morphologically cryptic species ([Table 1](#)).

To increase species identification reliability, a standardisation of the widely divergent analytical methods for species assignments ([Borkent, 2021](#)) and a unifying framework to understand and manage invasions have been repeatedly requested ([Blackburn et al., 2011](#); [Sakai et al., 2001](#)). Here we attempt to respond to these requests, and we have divided the study into two matching sections. The first part evaluates the efficiency of common analytical methods used for species and taxonomic assignments through a meta-analysis combining the outcomes of taxonomic studies conducted over the last 10 years. Here, we defined accurate analytical methods to discriminate species and OTUs at varying levels of divergences ([Fig. 1](#)). The second part provides a methodological framework using a combination of DNA barcoding for a single locus, morphometry and advanced taxonomy to develop effective taxonomic assignments and highlight the need for accurate taxonomic information in management plans of alien species, and particularly cryptic species introduced through the trade (see graphical abstract). We tested the combined taxonomic method on the brown frogs (*Rana* sp.) imported into the Republic of Korea through the legal international trade, and potentially masking the risk of biological invasions by species from a genus that is both genetically and morphologically cryptic. Thus, our implementation of the proposed integrative morphometric and bioinformatics workflow on the traded cryptic brown frogs has two objectives: (1) to identify the cryptic species, classify the OTUs and trace the uncertain origins of traded specimens; (2) to identify key morphometric trait(s) useful for species identification, and propose a general key morphometric trait for northeast Asian *Rana*.

2. Materials & methods

2.1. Sampling and datasets preparation

For the first part of study, we assembled already published data from the last 10 years, including peer-reviewed articles related to taxonomy ($n = 57$). For the second part of study, we collected 109 live Brown frogs *Rana* from a legal amphibian market in northern Republic of Korea in May 2016, 2017 and 2019 ([Table S2](#)). The traded live specimens were imported for food and medicinal purposes, and officially originate from 'Gillum Seong' Mountain, Jilin province, eastern People's Republic of China ($N40.95^\circ$, $E125.25^\circ$). They are legally imported into the Republic of Korea under the name '*Rana dybowskii*'.

We included two types of datasets for species assignments: (i) DNA sequence, and (ii) morphology. For species assignments with DNA sequences, we barcoded the 187 *Rana* samples originating from the market sampled between 2016, 2017 and 2019 with the universal 16S rRNA gene marker. After assessing the quality of the sequences, the final dataset included 171 *Rana* sequences ([Table S2](#)). For species assignment through morphometry, we analysed the 108 live samples collected from the trade in 2019, and for a comparison, we added 100 additional *Rana* specimens from the Republic of Korea (three species: 55 females, 43 males and 2 unidentified individuals; [Table S3](#)) obtained from the collection of the Natural History Museum of Ewha Womans University, Republic of Korea (Museum catalogue numbers provided in [Table S3](#); [Shin et al., 2020](#)).

Table 1

Pairwise comparison for conservatism of comparative species assignment methods commonly used for barcoding-based studies between 2010 and 2020. The mean of effect size (Cohen's d) and calculated strength of association (r) values highlight the presence of variation in conservatism within each method when determine species crypticity.

Pairwise comparison for efficiency between taxonomic assignment methods	Effect size (Cohen's d)	HPD 95% lower	HPD 95% upper	Strength of association (r)	Cohen's interpretation of r (0.1–1.0)
Coalescent (GMYC/bPTP) vs. morphology	0.624	0.537	0.709	0.298	Small effect
Coalescent (sGMYC) vs. distance (ABGD)	0.096	0.022	0.166	0.048	No effect
Coalescent (mGYC) vs. distance (ABGD)	0.209	0.077	0.339	0.104	Small effect
Coalescent (bPTP) vs. distance (ABGD)	0.153	0.042	0.269	0.076	No effect
Coalescent (bPTP) vs. coalescent (sGMYC)	0.027	-0.006	0.058	0.013	No effect
Coalescent (mGYC) vs. coalescent (bPTP)	0.096	-0.096	0.283	0.057	No effect

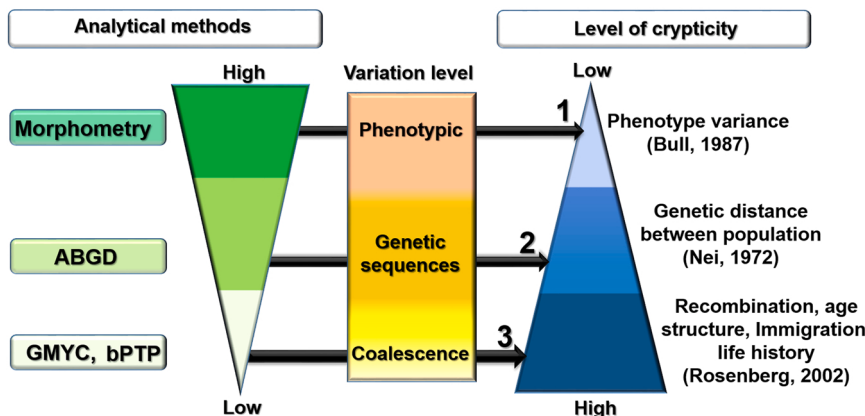
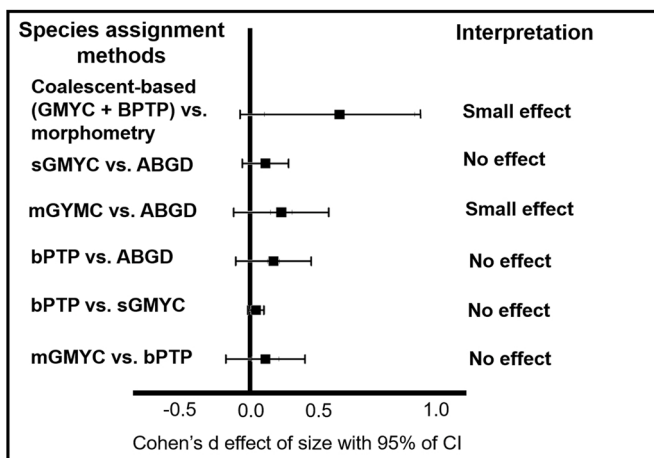


Fig. 1. The rank of efficiency of the popular analytical methods used to infer the different levels of cryptic diversity inferred from meta-analysis. The species delimitation methods were harvested from the literature and used in the meta-analyses (referring to Figs. S1–S6 in supplemental information). The interpretation on the strength of associations between pairwise species assignment methods is adapted from Cohen (1988), with a r index (0–1) indicating: $r = 0.1\text{--}0.3$ for a small effect; $r = 0.3\text{--}0.5$ for an intermediate effect and $r = 0.5\text{--}1.0$ for a strong effect. The numbering between 1 and 3 indicates three levels of probability for crypticity, from high to low, reconstructed from Bull (1987), Nei (1972), and Rosenberg et al. (2002): (1) indicates phenotypic crypticity, (2) indicates genetic sequence crypticity and (3) indicates crypticity at a deep level of the evolutionary process. The abbreviations used in species assignment methods are such as: Automatic Barcode Gap Discovery (ABGD), Bayesian implementation of the Poisson Tree Processes (bPTP), single-Generalised Mixed Yule Coalescent (sGMYC) and multi-Generalised Mixed Yule Coalescent (mGMYC).

2.2. Ethical guidelines

The specimens were purchased for consumption, originating from the legal trade, and therefore do not require permits. Due to the unknown origin of the brown frogs from the trade, the specimens were not released to the wild. All the individuals were immediately processed in the laboratory following the least pain-inflicting standard protocol of invasive amphibian eradication (Orchard, 2011). We first swabbed them (cotton-tipped swab; 16H22, Medical Wire; Corsham, UK) for genetic materials, and euthanasia was conducted through cooling and then freezing as the nervous system related to pain in amphibians is not triggered in this condition (Shine et al., 2015). Here, no experiments on animals were conducted in the lab, and molecular analyses such as Polymerase Chain Reaction (PCR) and sequencing do not warrant any permit based on guidelines of EWHA Institutional Animal Care and Use Committee (IACUC), Republic of Korea, and the ethical recommendations of the College of Biology and the Environment at Nanjing Forestry University.

2.3. Meta-analysis: comparison of efficiency between popular analytical methods for taxonomic assignments

In the first section, we focused on evaluating the efficiency of common analytical methods used for taxonomic assignments across the tree of life. To evaluate the variation in the sensitivity of these analytical methods, we compared published studies from the last 10 years (2010–2020) of taxonomic and barcoding-based studies through a meta-analysis. Here, we conducted a cross-study comparison on the pattern of sensitivity or efficiency (referred to as conservatism in determining crypticity) of popular analytical methods for species assignments such as external morphometry, and phylogenetic species concept approach with species delimitation, including

genetic distance-based, Automatic Barcoding Gap Discovery (ABGD) and coalescent-based analyses such as Generalised Mixed Yule Coalescent (GMYC) and Bayesian-Poisson Tree Processes (bPTP) (Fig. 1 and Forest plots in Figs. S1-S6). Each analytical method (i.e. morphometry, species delimitation modelling) operates following a specific statistical design or algorithm and thus provides different phylogenetic resolution regarding the number of possible OTU.

For the meta-analysis, we compiled the peer-reviewed articles published between 2010 and 2020 that applied comparative species delimitation to solve species boundary questions. Our criterion for the articles needed for the synthesis contained the use of species delimitation method with a single or/and multi-locus data, and the subjects including animals, plants, fungi, and protists. Hence, our search was conducted using Google Scholar with the following key words: 'species delimitation', 'coalescent', 'barcoding', 'species assignment', 'cryptic diversity', 'ABGD', 'GMYC', 'PTP', 'BFD' and 'genetic distance'. The final collection resulted in 57 peer-reviewed articles (Table S4; Figs. S1-S6).

To analyse the efficiency of species assignment methods (morphometry, ABGD, sGMYC, mGMYC and bPTP), we quantified the performance of each comparative species assignment method in isolating cryptic OTUs. We selected studies that compared morphometry, genetic barcoding and species delimitation approaches, and computed the mean difference effect size between subgroups containing six pairs of comparative species assignment methods: (a) coalescence vs. morphometry ($n = 10$, n participants = 9780), (b) coalescence sGMYC vs. distance-method ABGD ($n = 40$, n participants = 68204), (c) coalescence mGMYC vs. distance-method ABGD ($n = 10$, n participants = 4715), (d) coalescence bPTP vs. distance-method ABGD (n studies = 32, n participants = 57560), (e) coalescence bPTP vs. coalescence sGMYC (n studies = 33, n participants = 33712) and (f) coalescence mGMYC vs. coalescent bPTP (n studies = 13, n participants = 3858). Here the participants in each subgroup reflect the accumulated number of cryptic OTUs that was estimated from each pair of comparative methods (subgroups a - f; Table S4 and Figs. S1-S6).

To synthesised the data from the articles collected, we constructed forest plot using Review Manager (RevMan) v.5.4.1 (The Cochrane Collaboration, 2020). Our synthesis was conducted under the null hypothesis that more conservative methods will result in a smaller number of OTUs. To test the overall effects of size between comparative species assignments methods (subgroups a - f), we assigned the putatively conservative method such as morphometry and distance-based species delimitation as control and the putatively less conservative method as experimental in our data comparison table in RevMan v. 5.4.1. To measure the performance of each comparative species assignment method in identifying cryptic OTUs, we measured the odd ratio, risk ratio and risk differences occurring in all six pairs of comparative species assignment (Table S4). Based on the difference between the means of odd ratio obtained from the sampling results of each event from extracted articles, we measured the mean effect size using a t-test (Cohen's d statistic; Cohen, 1988). Here we computed the strength of association (r) among the pairwise comparison with both values later used to index the conservatism of each method. We interpreted the strength of sensitivity for each pairwise comparison based on the interval for (r) proposed by Cohen (1988) with a (r) value ranging from 0.1 to 0.3 indicating a small effect, a r value ranging from 0.3 to 0.5 indicating an intermediate effect and a r value ranging from 0.5 to 1.0 indicating a strong effect (see Cohen's d interpretation in Fig. 1; Table 1).

2.4. Integrative workflow to identify cryptic species from the amphibian trade

In the second section, we focused on addressing crypticity in taxonomy and routes of used by the amphibian trade. To do so, we tested an integrative workflow consisting of morphometric and barcoding bioinformatics for species assignment, and origin-tracing methods for the traded brow frogs (graphical abstract). The combined analytical methods consisted of three separate workflows, named as species assignment 1–3 (see subtopics below).

2.4.1. Laboratory protocol and digital images

Upon collection and euthanasia by cooling and freezing, we ensured that all specimens were dead. We photographed all 109 *Rana* specimens acquired from the trade ($n = 109$) in 2019 before they were frozen and stiff, using a horizontal tripod and a digital camera (DSLR, Nikon D80, AF-S DX Zoom Nikkor ED 18–135 mm F3.5–5.6 G; SB-R200, Nikon; Tokyo, Japan). We photographed each individual from three angles: dorsal, ventral and lateral, with a scale for calibration. All photographs were taken with the aperture of the camera lens parallel to the plane on which the frogs were set-up to avoid parallaxes during downstream measurements. We then preserved all specimens in 100% alcohol for a long-term storage. For further comparison, we repeated the procedure with 100 museum specimens representative of two native Korean *Rana* species: *R. coreana* and *R. uenoii* originating from the collection of the Natural History Museum of EWHA Womans University, Republic of Korea (Museum catalogue numbers provided Table S3; Shin et al., 2020).

2.4.2. Molecular analyses

The total genomic DNA was extracted from buccal swab samples using Qiagen DNeasy Blood and Tissue kit (QIAGEN Group, Hilden, Germany) according to the manufacturer's protocol. In total, we combined 176 samples from 2016 ($n = 53$), 2017 ($n = 26$) and 2019 ($n = 99$). The samples from 2016 and 2017 were not photographed and their bodies were not preserved. For all samples, we amplified a 550 bp-long fragment from the 16S rRNA mitochondrial gene (mtDNA) using the amphibian universal barcoding markers 16-SAL and 16-SBH (Vences et al., 2005). The selection of these primers was based on the value of the gene fragments for phylogenetic inference, phylogeography, and prior successful use in taxonomic studies on *Rana* (Vences et al., 2013). We prepared all PCR in 20- μ L volumes of total reaction, each containing approximately 50 ng of genomic DNA, with a final concentrations of other PCR reagents of 0.125 μ M for each forward and reverse primer, 1x Ex taq Buffer (Takara, Shiga, Japan), 0.2 mM of dNTPs Mix (Takara; Shiga, Japan), 1.875 mM of magnesium chloride ($MgCl_2$), 0.1 unit/ μ L of Ex taq (HR001A, Takara; Shiga, Japan) and double distilled water to make up the total volume. PCR amplifications for 16S rRNA gene fragment were conducted with an initial denaturation of 95 °C for 5 min

followed by 35 cycles at 94 °C for 30 s, 55 °C for 30 s, 72 °C for 60 s, and a final elongation at 72 °C for 10 min. All amplifications were conducted with a PCR machine SimpliAmp™ Thermal Cycler (Cat. no A24811, Applied Biosystems; USA). All PCR amplicons were purified and sequenced for both forward and reverse strands on an ABI platform (CosmoGenetech Company Co., Ltd.; Seoul, Republic of Korea).

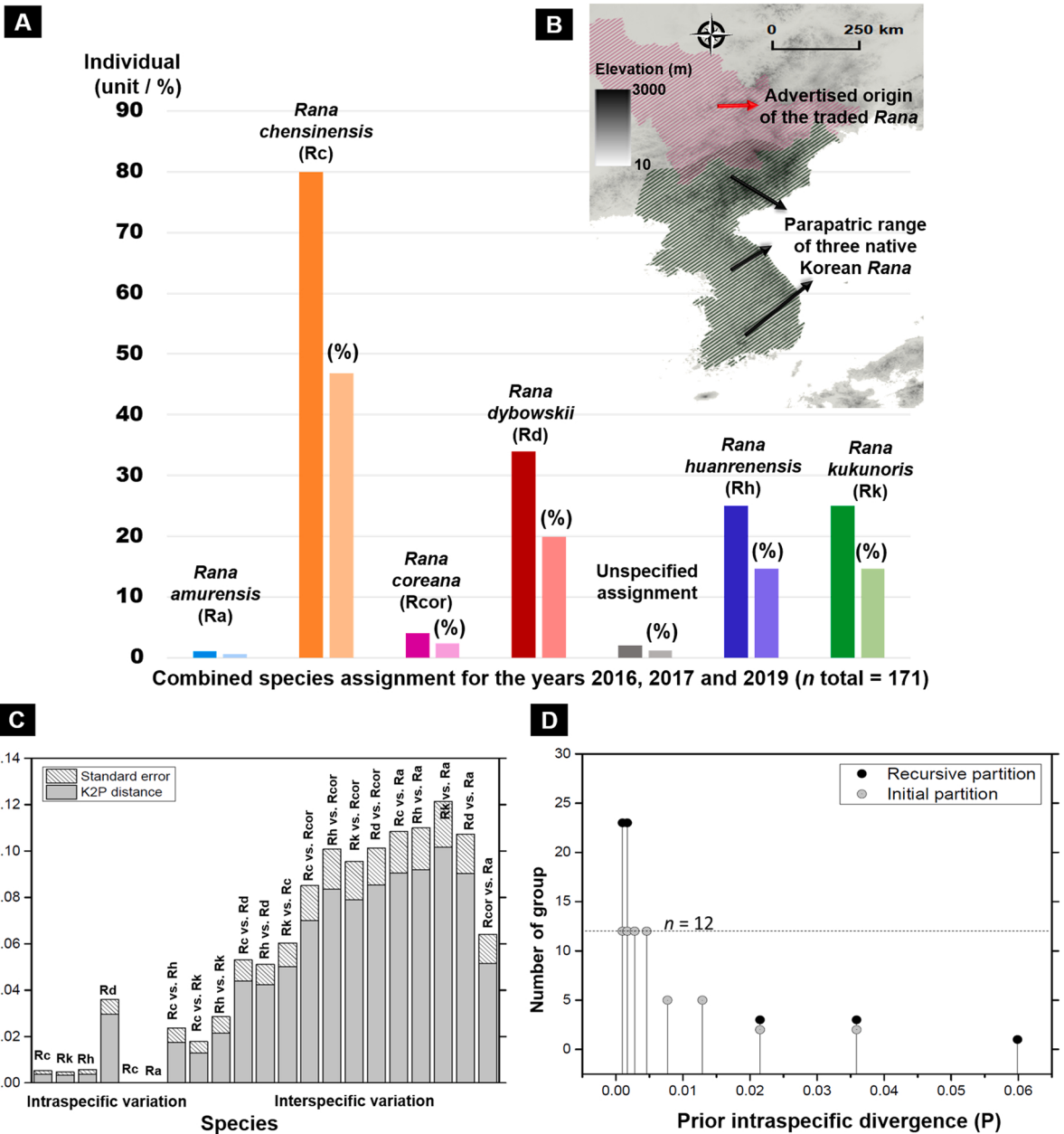


Fig. 2. Screening of 171 brown frogs (*Rana*) imported into the Republic of Korea through the wildlife trade using DNA sequencing. (A) The number of individuals per species among *Rana* sourced from the trade collected between 2016 and 2019, identified using conventional DNA barcoding 16S rRNA (385 bp) and screened using BLAST. The bar chart in (A) is colour coded by species, with the darker colour indicating the number of individuals and the lighter colour indicating the frequency of individuals (%) of that species compared to the total number of specimens. (B) Distribution range of native Korean *Rana* (dark grey shade) and the origin of individuals from the trade as reported by the seller (red shade). The distribution ranges of native Korean *Rana* are downloaded from the IUCN Red List (www.iucnredlist.org). (C) Genetic distance among and between species. The genetic distances follow the same pattern of barcoding gap where the mean of interspecific variation is segregated from the mean of intraspecific variation. (D) Estimations of the most-likely number of operational taxonomic unit (OTU, n = 12) through a primary species delimitation with the Automatic Barcode Gap Discovery (ABGD) method.

2.4.3. Species assignment 1: DNA barcoding with distance-method

To analyse the genetic data collected from the traded specimens, we first barcoded all samples with the 16S rRNA gene fragments ($n = 171$; Table S2; Fig. 2A). To search for most homologous sequence, we conducted an analysis of similarity using Blastall-Blastn tool

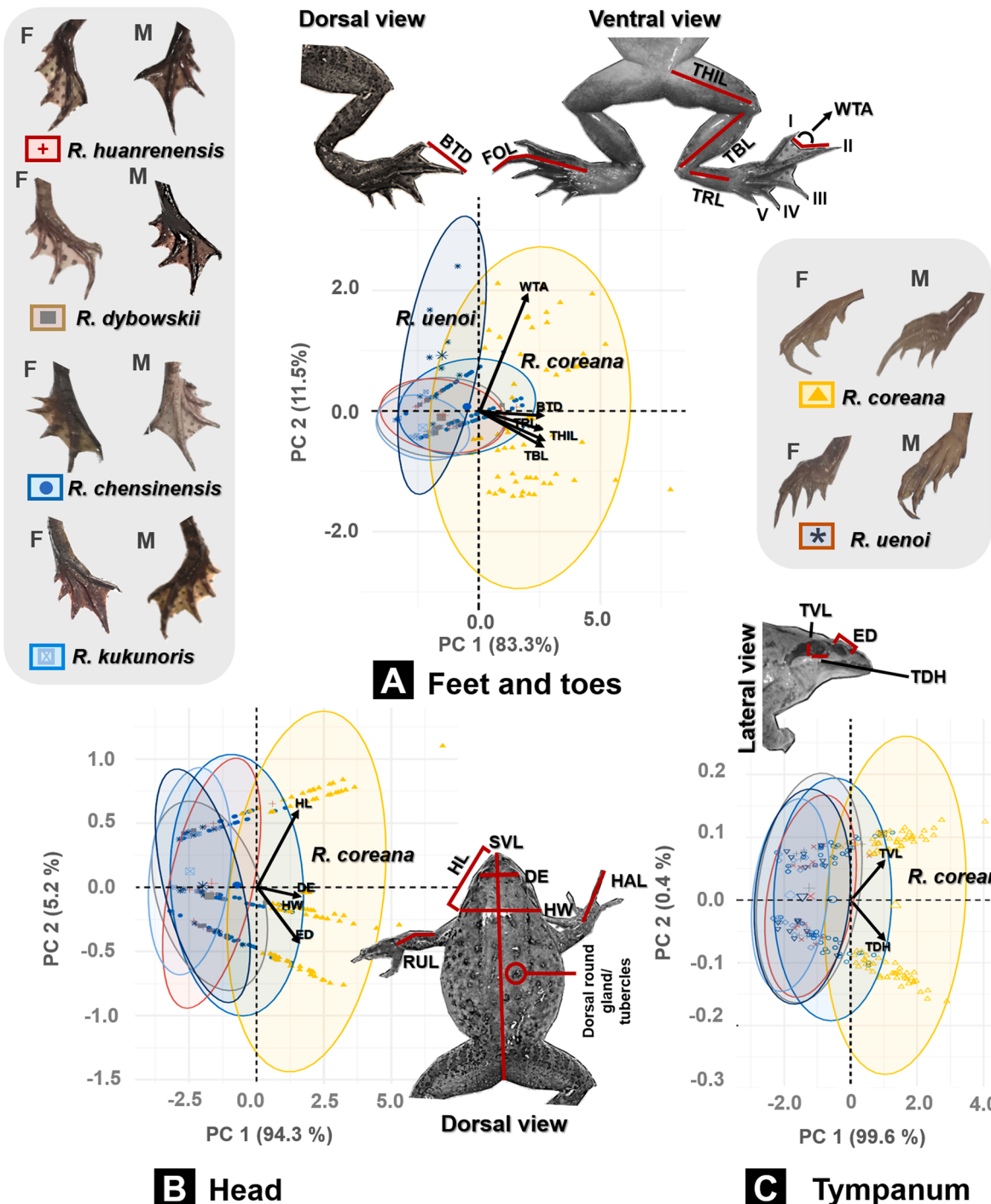


Fig. 3. Key morphometric traits for identification of phenotypically cryptic brown frogs (*Rana*) in northeast Asia. The PCA biplots show the PC scores and morphometric measurements for 208 specimens originating from the wildlife trade and supplemented by a museum collection (EWNHM) as representative of the native Korean *Rana* species (*R. coreana* and *R. uenoi*). PC scores are marked by the species-specific coloured dots for each genetically identified *Rana* species. The arrows indicate the vector of each morphometric variable. The further a variable is from the PC origin, the higher the influence of the trait on the PC. The statistical analyses related to morphology are in Supplementary Tables S5-S10.

(Altschul et al., 1990). Next, we computed the pairwise genetic distance (*p-distance*) to calculate the level of overlap (total and 90%) between intra-specific and inter-specific genetic distances through 100 bootstraps using Kimura 2 Parameter (K2P; Kimura, 1980) in MEGA v.6.0 (Tamura et al., 2013). To trace the presence of discrete barcoding gaps, we plotted the maximum intra-specific distance against the minimum inter-specific distance. To specify a species-level assignment using the barcode gaps, the means of the inter-specific distance must be higher than the means of intraspecific distance (Candek and Kuntner, 2014). We then proceeded to the species delimitation using the ABGD (Puillandre et al., 2012). The program ABGD predicts the most probable number of OTUs through a distance-threshold algorithm (Jörger et al., 2012; Puckridge et al., 2013). The analysis was run through the web server <https://bioinfo.mnhn.fr/abi/public/abgd/abgdweb.html>.

2.4.4. Species assignment 2: morphometric using photographs

There is so far no general identification key matching morphology and species for northeast Asian species. Some morphological criteria are used to differentiate between some locally sympatric species, but none of the key can be used for the region in general, and the current knowledge is especially inadequate to identify species originating from distant localities through the trade (Table S1). Hence, we were not, and could not, compare the performance between morphological assignment and molecular assignments. Rather, we integrated the morphological assignment within the phylogenetic comparative trait in order to understand the morphological patterns within the species traded. We measured the trade-sourced and museum voucher specimens ($n = 208$) based on the following morphological variables (one meristic and 14 morphometric): presence of round dorsal glands, snout-vent length (SVL), maximum head-length (HL), maximum head-width (HW), horizontal eye diameter (ED), distance between the eyes (DE), radio-ulna length (RUL), tibia length (TBL), tarsus length (TRL), thigh length (THL), hand length (HAL), foot length (FOL), horizontal tympanum diameter (TDH), and vertical tympanum diameter (TDV). We also measured the distance between toes I and II (BTD) and the angle made by the webbing between webbed toes I and II (WTA) (Fig. 3). Particularly for the toe webbing morphology, we followed the descriptions from Savage (1975), Song et al. (2006) and Matsui (2014) to determine the BTD and WTA variables.

2.4.5. Statistical analyses for morphometry

We standardised the 14 continuous morphometric variables for size variation by dividing them by the SVL of the same individual. Each variable was determined to be normally distributed through the observation of the QQ-plots. We then analysed the effect of the categorical variables against the continuous morphometric variables with an Analysis of Covariance (ANCOVA) with all 14 morphometric variables set as dependent variables and species and sex as categorical independent variable. This test indicated that sex did not have a significant effect on the morphometric variables ($df = 1$; $F = 0.042$; $p = 0.485$; see details in Table S5-S6), and therefore we did not discriminate by sex for subsequent analyses.

We then tested for correlation between the 14 morphological variables for the 208 individuals through a Pearson's correlation test. As all variables were highly correlated (Pearson test; $0.58 < R < 1$; $p < 0.0001$), we ran a principal component analysis (PCA) to obtain the Principal Components (PCs) most representative of the morphometric variables measured. As we could not measure WTA for all individuals (n missing data = 31), we tested the percentage of variance expressed by each of the PCs with WTA (variables $n = 14$, individuals $n = 176$) and without WTA (variables $n = 13$, individuals $n = 208$). After comparing the variance, we selected the first dataset that included WTA for further analyses despite a lower number of individuals due to the high percentage of variance expressed (PC1 = 84.6% and PC2 = 6.3%).

We then searched for key morphological traits that can be used to distinguish *Rana* individuals by their evolutionary unit. To increase the resolution of the morphometric variables, we split the data into three independent datasets for all samples, purchased from the market and from the museum: feet and toes ($n = 176$), head ($n = 208$) and tympanum ($n = 208$). We analysed each dataset through independent PCAs. To assess for variations within each of the three datasets, we conducted a one-way ANOVAs with PCs as dependent variables and morphological variables as independent variables, followed by Tukey post-hoc tests (Fig. S8). All statistical analyses were conducted with the packages Cars, STAT and factoextra (Josse and Husson, 2016; Kostov et al., 2013) in R v.3.6.3 and RStudio (R Core Team, 2020).

We determined the most distinctive continuous variable for species identification through the reconstruction of ancestral morphological trait. We based this analysis on the morphology of feet and toes as it is a visible character that can be used to differentiate between some *Rana* species (Song et al., 2006). In addition, this trait is likely species specific due to the evolutionary pressure resulting from the locomotive performance of anurans (Kosmala et al., 2017). To do so, we reconstructed a STARBEAST species tree with BEAST v.2.6.1 (Bouckaert et al., 2019). We then calibrated the tree with the combination of an uncorrelated relaxed clock and Yule tree priors following a normal distribution. We enforced two calibrations points taken from: (1) the vicariance of the *R. chensinensis* clade on the southern Qinghai-Tibetan Plateau (c.18.0 Mya: Zhou et al., 2012) and (2) the emergence of the *Rana dybowskii* clade, corresponding to the disconnection between Hokkaido and Sakhalin Islands from the Eurasian continent (c. 0.8.55 Ma; Yang et al., 2017). We mapped the ancestral range of the morphological trait and analysed the trajectory of the trait evolution across time using the Brownian motion and the OU (Ornstein Uhlenbeck) model into the reconstructed species tree using the package phytols (Revell, 2012) in R v.3.6.3 and RStudio (R Core Team, 2020).

Finally, to test for morphological crypticity among *Rana* species, we ran a PCA on the morphometric dataset based on two related cladistics scenarios found in phylogeny and geographical distribution: polyphyletic and parapatric scenarios. We restricted the morphological dataset to species that are polyphyletic (*R. chensinensis* $n = 56$, *R. kukunoris* $n = 15$ and *R. huanrenensis* $n = 18$; see Fig. 5B), and species that are distributed in parapatry (*R. dybowskii* $n = 12$, *R. huanrenensis* $n = 18$, *R. uenoi* $n = 10$, *R. coreana* $n = 58$; see distribution map in Fig. 5C). To test the significance differences among the most influential trait suggested by the PCAs in the two scenarios, we conducted a one-way ANOVA with the "key morphological trait" as dependent variables and species as the independent

variable.

2.4.6. Species assignment 3: comparative species delimitations using the coalescent-method

We further analysed the dataset of *Rana* sourced from the trade ($n = 171$) and barcoded with the 16S rRNA gene fragment (385 bp) through a comparative species delimitation model to determine the most likely number of OTUs. This analysis was conducted to detect the presence of cryptic ESU. In this comparative analysis, we divided species-level identification into two categories: first using a conventional genetic similarities and genetic distance approach (BLAST, ABGD) and second using a tree coalescent approach (GMYC and bPTP). We then evaluated the cryptic lineages identified by each species delimitation method and compared the results of the estimated number of OTUs.

2.4.7. Reconstruction of the Bayesian poisson tree processes (bPTP) tree

First, we tested for the best model of sequence evolution using the Bayesian Information Criterion (BIC) algorithm in jModeltest v.2.0 (Darriba et al., 2015). We obtained TrNef+G as best model of sequence evolution based on the smallest value of the BIC (-lnL = 963.7886). We then reconstructed two ultrametric trees using the dataset with independent analyses using BEAST v.2.5.2 (Bouckaert et al., 2019). For both ultrametric trees, we independently selected a lognormal molecular clock with no zero branch lengths. We also selected a coalescent constant for the tree prior and run the two analyses with 10 million MCMC chains until the trees converged. We summarised the ultrametric trees into a Maximum Clade Credibility (MCC) tree with a posterior probability of clades greater than 0.5 and discarded the first 20% of trees as burn-in. We evaluated the Effective Sample Size (ESS) parameters of the MCC tree with Tracer v.1.6 (Bouckaert et al., 2019). We ensured the ESS value for each parameter reached 200 for a better sampling accuracy (Yu et al., 2017). We implemented the MCC tree for the reconstruction of species delimitation trees based on coalescent-based approaches, using a Poisson Tree Processes (PTP; Zhang et al., 2013), and the species delimitation models were run on the web server (<https://species-hits.org/>).

2.4.8. Reconstruction of single threshold- Generalised mixed yule coalescence method tree

Here, using the dataset of *Rana* sourced from the trade ($n = 171$), we first calibrated the tree with two different priors: the Yule prior and the constant coalescent prior under an uncorrelated lognormal relaxed clock model. We enforced the two calibration points previously used in the time tree generated for the ancestral trait reconstruction and set the calibrations with normal distributions. We constructed the tree and scaled the time using BEAST v.2.4.8 (Bouckaert et al., 2014) and ran two independent analyses with the MCMC chain for 20 million generations. The convergence of the run was examined with Tracer v.1.7 (Rambaut et al., 2018) and all parameters reached the ESS value of 200. The trees were combined with LogCombiner and annotated with TreeAnnotator (Bouckaert et al., 2019). We estimated the threshold time and species boundary of our calibrated tree using the s-GMYC method with the packages split and phytools (Revell, 2012) in R v.3.6.3 and RStudio (R Core Team, 2020).

2.4.9. Selection of best-supported OTUs scheme with path sampling analysis

To verify the presence of cryptic OTUs we set a null hypothesis where the ideal number of OTUs should be comparable to the number of described species ($n = 6$; Fig. 2A) based on the BLAST results. The alternative hypothesis was that if the estimation of OTU is higher than the number of described species in BLAST, the results would indicate the presence of supernumerary evolutionary significant unit within the traded *Rana*. To do so, we simulated all estimated models (BLAST, ABGD, sGMYC and bPTP) with a Bayes Factor Delimitation (BFD) species tree model (Grummer et al., 2014) using the SNAPP package implemented in BEAST v.2.6.1 (Bouckaert et al., 2019). This is important to obtain the most accurate number and the patterns of OTUs to infer the presence of cryptic lineages and to help reconstruct the origin of traded individuals within the phylogenetic tree. We first re-assigned the species limits of the OTUs from the four models and ran each of them with the BFD model in BEAUti2 under the SNAPP template. We selected a coalescent rate of 10, and set gamma as rate prior with a mean value of 0.05 and set the alpha value to 0.086, beta value to 1.842 and kappa of 1. We calculated the alpha and beta values based on the following formula: $\alpha = (M^2)/[M_2 - M^2]$; and, $\beta = [M_2 - M^2]/M$, where M is mean value of gamma 0.05. We chose a mutation model and selected the log-likelihood correction option. To obtain the range of tree heights (in expected substitutions per site), we calculated the substitution sites of the genes with 0.05% rates per 1000 bp nucleotides as estimated by the model selection program. To set the parameter lambda, we estimated the value based on the lambda prior settings provided by the SNAPP module, where the estimation on the range of species height compared to the size number of OTUs per scheme. We ran each scheme with MCMC samplings for 10 million generations with a burn-in of 500,000.

The convergence of final run for each scheme was ensured by visualizing its MCMC outputs (ESS > 200) with Tracer v.1.7.1 (Rambaut et al., 2018). The MCC tree topology and ancestral population size parameter (theta) values were generated from each model, for further evaluation of the species boundary through the selection of best-fit OTUs scheme.

To evaluate the OTU schemes ran through the BFD, we assessed the model support values through a path sampling analysis using Path Sampler, an application embedded in BEAST v.2.61 (Bouckaert et al., 2019). We ran each model sampler for 1 million iterations with seven steps of marginal likelihood and a burn-in of 100,000. We obtained the value of marginal Likelihood Estimation (MLE) for each model where the highest value of MLE indicates the best support for the model. We ranked from best to lowest supported models based on the MLE obtained. We also compared the value of the Bayes Factor (BF) determinant (Baele et al., 2013). We calculated the BF with the following formula: $BF = 2 \times [\text{MLE value of selected model} - (\text{MLE value of default model})]$. We assigned the BLAST model as a default model for any species assignment, and the species delimitation models were tested as alternative models. We selected the best model of species delimitation using the positive and negative value of BF. If the difference value is positive, then BF is in favour of the default model, whereas negative difference value would indicate BF in favour of the alternative models.

2.4.10. Trade origins: phylogenetic tree and Bayesian clustering

To ascertain the origin of the *Rana* samples collected from the trade, we conducted a phylogeographic analysis. Here, using the classified group of OTUs from best-supported ABGD model that we have determined using BFD modelling (Fig. 6), we reconstructed a 16S rRNA gene barcoding-based Bayesian Inference (BI) tree comprising the *Rana* specimens sourced from the trade ($n = 171$) and *Rana* samples sourced from natural population with known localities (Table S2). Due to the commonality of 16S rRNA gene marker, we obtained additional homologous sequences from Genbank with known locality, representing various *Rana* species distributed across northeastern Asia and assigned as ‘control’ sequences to retrace the geographic origins of our *Rana* specimens originating from the trade. The ‘control’ sequences included the homologous sequences of pre-identified samples from six species: *R. amurensis*, *R. dybowskii*, *R. huanrenensis*, *R. kukunoris*, *R. chensinensis*, *R. uenoi* and *R. coreana* distributed across northeastern Asia (Yang et al., 2010; Jeong et al., 2013; Zhou et al., 2015; Dong et al., 2016; Li et al., 2016; Othman et al., 2020b; Table S2). This final dataset resulted in 230 sequences for the 16S rRNA gene fragment (386 bp) isolated from traded specimens ($n = 171$), along with our ‘control’ sequences ($n = 59$).

To build the BI tree, we first determined HKY + G to be the best nucleotide substitution model for the partial non-coding 16S rRNA gene barcode using Mr. Bayes v. 3.2.6 (Huelsenbeck and Ronquist, 2001) instead of relying on the fixed ‘mr. bayes’ parameter using PartitionFinder v. 2.1.1 (Lanfear et al., 2017). We then computed the tree reconstruction for 30 million generations of MCMC using four parallel chains, where the chains were sampled every 1000 generation until the standard deviation of the split frequencies reached a value lower than 0.01.

Finally, we examined the origin of samples sourced from the trade. To do so, we mapped the possible origins of the samples obtained from the trade based on the clustering of the clades recovered with the ‘control’ *Rana* in the BI tree. The distribution of the *Rana* obtained from the trade was pinpointed on the map based on the information about the OTUs obtained from the best-supported species delimitation model (ABGD, n OTU = 12, n taxa = 171).

3. Results

3.1. Variation in efficiency of analytical methods to isolate OTUs

Our cross-study comparisons for the peer-reviewed articles ($n = 57$; refer to forest plots in supplementary Figs. S1-S6) published over the last 10 years (2010–2020) demonstrated a significant variation in sensitivity among the different methods of species assignment. Computed mean-difference effect size for the meta-analysis showed that morphometry is the most conservative (or least sensitive) method in specifying the number of OTUs, followed by the distance-based and coalescent-based species delimitation methods (Table 1, Fig. 1). First, a small mean size effect supported that morphometry was more conservative in species assignment in comparison with the coalescent approach (Cohen’s $d = 0.624$ [HPD 95%: 0.537 – 0.709]; r value: 0.298; Table 1, Fig. 1) in determining cryptic OTUs. Second, we also demonstrated that a variation between the distance-based species delimitation (ABGD) and the coalescent-based species delimitation (GMYC and PTP) with a small effect indicates that the former was more conservative than the latter (Cohen’s $d = 0.209$ [HPD 95%: 0.077 – 0.339]; r value: 0.104; Table 1, Fig. 1). We did not find any size effect among the different methods of coalescent-based approach.

3.2. Integrative morphometry and barcoding bioinformatics for the amphibian trade

In general, our application of integrative workflow using morphometric and barcoding bioinformatics for taxonomic assignments and trade origin-tracing addressed the presence of cryptic lineages in the *Rana* sp. imported into the Republic of Korea ($n = 171$), and retraced the most probably origins for all traded specimens. Our supplemental screening using model-based species delimitation was able to determine the best OTUs scheme among the three main species assignment methods (distance-based barcoding, morphometry and coalescent-based species delimitations) and improved the adequacy of single locus barcoding using the 16S rRNA gene. Furthermore, merging the information on OTUs with the phylogenetic tree efficiently helped resolve the putative origin of the traded *Rana*. The details of each species assignment method for *Rana* specimens originating from the trade are such as follows.

3.2.1. Species assignment 1: DNA barcoding with distance-method

The screening of sequence similarity with BLAST grouped brown frogs originating from the trade into six well-defined species (Fig. 2A). Two species were however not accurately assigned because the randomised BLAST resulted in more than one most homologous species (Fig. 2A). We marked these two individuals as ‘unspecified assignments’ and we kept them for further species identification through a more sophisticated species delimitation approach. Most traded brown frogs (n total = 171 individuals) between 2017 and 2019 were *Rana chensinensis* (total count: 46.78%; Fig. 2A and S7), followed by *R. dybowskii* (19.88%; Fig. 2A and S7). The pattern of intra- and inter-species genetic divergence displayed barcoding gaps within the 16S rRNA gene sequences of the traded *Rana*, indicated by a higher value of interspecific distance than the maximum intraspecific distance (see K2P graph pattern on intra and inter-specific distance; Fig. 2B). The two unassigned individuals through the primary screening with BLAST were here identified as *R. dybowskii* ($n = 1$; interspecific divergence of 2.81% with *R. huanrenensis*; Fig. 2B), and *R. kukunoris* ($n = 1$; interspecific divergence of 3.75% with *R. chensinensis*; Fig. 2B). Based on the K2P genetic distance method, the specimens were assigned to *R. amurensis* ($n = 1$; 0.58%; Fig. 2B), *R. chensinensis* ($n = 81$; 47.37%; Fig. 2B), *R. coreana* ($n = 4$; 2.34%; Fig. 2B), *R. dybowskii* ($n = 32$; 18.71%; Fig. 2C), *R. huanrenensis* ($n = 27$; 15.79%; Fig. 2) and *R. kukunoris* ($n = 24$; 14.04%; Fig. 2B).

The distance-based species delimitation with ABGD delineated between 3 and 24 OTUs among the *Rana* originating from the trade

($n = 171$; Fig. 2C). The prior maximum distance recorded a high consistency on the second, third and fourth partitions models, which resulted on 12 OTUs as the most consistent estimates (referring to the range of prior maximal distance; Fig. 2C).

3.2.2. Species assignment 2: comparative morphometry-phylogenetic traits

The PCA on all 15 morphometric variables (see result in Fig. S8) of *Rana* specimens from the trade and the museum collection ($n = 208$) indicated that tibia length (TBL) and the angle made by webbing between webbed toes I and II (WTA) principally loaded in PC1, explaining 84.6% of the variance (Fig. S8).

The presence of dorsal round glands, the horizontal tympanum diameter (TDH) and the vertical tympanum diameter (TVL) principally loaded in PC2, which explained 6.3% of the variance (Fig. S8).

The loading values extracted for feet and toes showed that TBL and WTA carried the most weight for the principal component 1 (PC1: 83.3%; Fig. 3A), resulting in *R. coreana* being clearly distinct from *R. uenoii* and other *Rana* originating from the trade (PC2: 11.5%; Fig. 3A). Levene's test for homogeneity of variance indicated a high variability in WTA ($df = 5; F = 17.88; p < 0.0001$) and TBL ($df = 5; F = 5.78; p < 0.0001$) across the traded and museum *Rana* specimens. The head length (HL) and eyes distance (ED) principally loaded in the PC1 and were the most influential characters related to head measurements, here as well helping to distinguish *R. coreana* (PC1: 94.3%) from the other *Rana* species (PC2: 94.3%; Fig. 3B). We also found significant variations in HL (ANOVA; $df = 5; F = 3.69, p = 0.0034$) and ED (ANOVA; $df = 5; F = 2.69; p = 0.02$) across all species. The PCs representative of the vertical and horizontal tympanum diameters also set *R. coreana* apart (PC1 = 99.6%) from the rest of the species (PC2 = 0.4%; Fig. 3C), with TDH significantly different (ANOVA; $df = 5, F = 2.32, p = 0.005$) and TVL close to be significantly different (ANOVA; $df = 5, F = 2.08, p = 0.07$) across the species.

Comparison of body proportions showed no significant differences between morphometric variables related to the feet and toes,

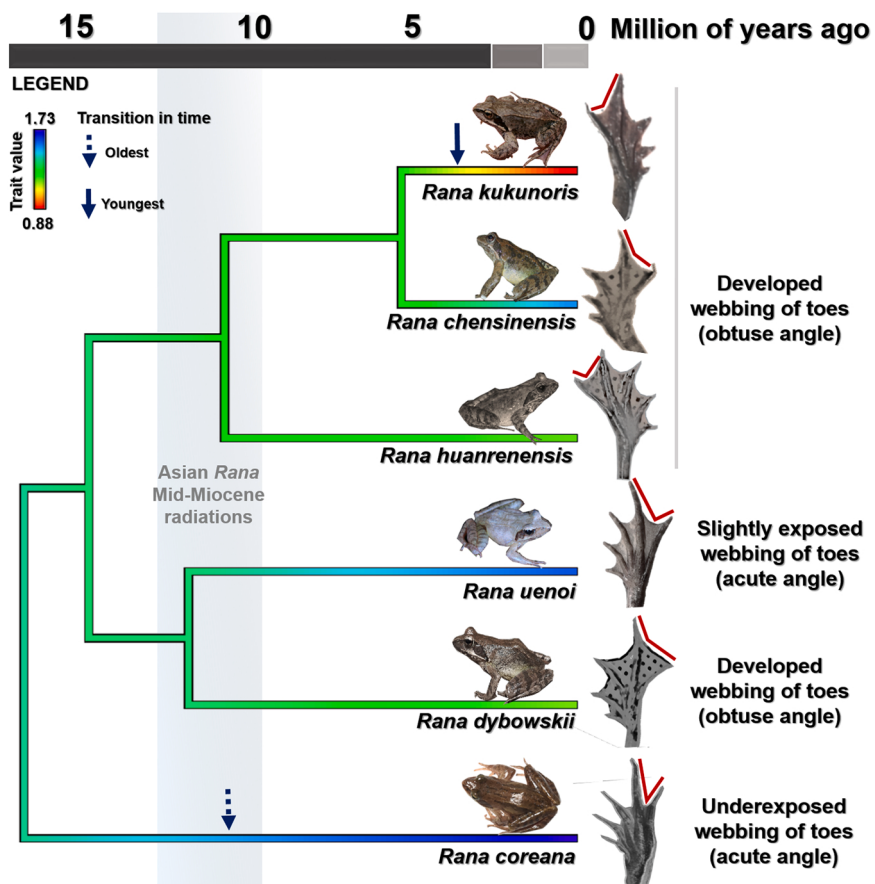


Fig. 4. Phenotypic evolution of toe webbing in selected northeast Asian *Rana* since the Miocene. The ancestral range reconstruction from the calibrated species tree including 181 individuals includes six taxa from northeast Asian *Rana* (385 bp of 16S rRNA). The colour coding in the trait value indicates the rate of evolution in phenotypic trait related to the angle made by the webbing between webbed toes I and II (WTA). The species the closest to the ancestral character is *Rana coreana* and the derived character rose in *R. kukunoris*. The earliest and the most recent transition times for WTA character to evolve from the ancestral to the youngest clades mark on the tree time with straight dotted and solid arrows, respectively. The phenogram, model fitting and pattern of trait bursting divergence for the phenotypic evolution of WTA across the lineage is described in the supplementary Fig. S9.

head, and tympanum in all species of *Rana* (Tukey Test in Table S7 and Fig. S8). However, the WTA showed a large variance among the traits tested across species and enable the differentiation of the native Korean *Rana* from the phenotypically cryptic traded specimens (Fig. 3A and S8). Hence, we further focused on the phenotypic evolution of WTA in comparative morphology and phylogeny.

3.2.3. Evolution in trait related to toe webbing

The phenotypic variations in toe webbing in the northeastern brown frogs based on morphometric analyses were also supported by phylogenetic patterns. Phylogenetic trait and ancestral character reconstruction on the morphological traits related to the structure of toe webbings, corrected for individual size variation for WTA, showed a convergence across the clades of northeastern Asian *Rana*. The pattern of evolution of WTA was random, best-fitting the Brownian motion model ($\sigma^2 = 0.06$; genetic drift = 0 and log likelihood = 266.65; Fig. 4). *Rana coreana* was the most closely related clade to the ancestral toe webbing character, with the trait evolution rate

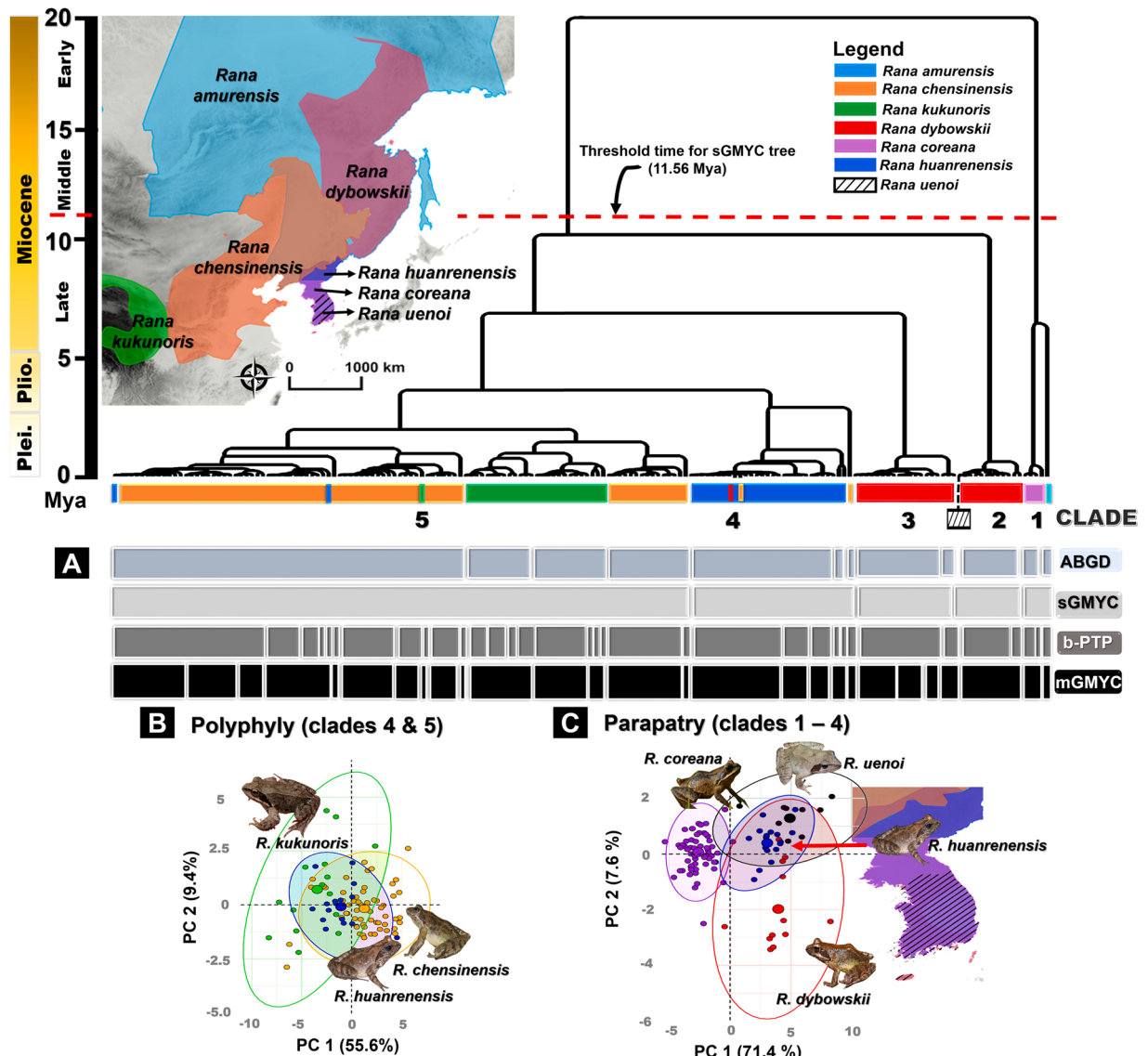


Fig. 5. Comparative species delimitations determining the OTUs on a calibrated timetree and matching comparative morphometry. (A) Comparative species delimitation based on the 16S rRNA gene barcode marker for 171 individuals of *Rana* originated from the trade determined by Automatic Barcode Gap (ABGD), General Mixed Yule Coalescent (GMYC) and Bayesian-Poisson Tree Process (bPTP) schemes. The partitions of the OTUs for each scheme is indicated below the tree nodes with specific colour gradients. The principal component analysis (PCA) for the 15 morphometric variables analysed for 208 individuals originating from the trade and a museum collection adjusted for (B) polyphyletic clades, and (C) parapatric clades (statistical analyses in Supplementary Tables S7 and S9). Each *Rana* clade is colour coded, matching with the colour of its range on the distributional map. The placement of *R. uenoi* in clade 2 was adapted from the Bayesian Inference tree and marked in the time tree (dashed box). The threshold time on the branch of the time tree is specific for the sGMYC method and the estimates are in the Supplementary Fig. S10.

estimated to be 1.73 times faster than in the other northeastern Asian *Rana*. In comparison, the species with the slowest trait evolution rate was *R. kukunoris* (rate = 0.88; confidence interval (CI): 0.96–1.88; n tree = 100; posterior probability = 0.94; Fig. 4). Additionally, a late bursting model supported a divergence in the characteristic of the toe webbings (Fig. S9). Here, the trait evolution pattern was also consistent with the divergence dating estimates for northeastern brown frogs, where *R. coreana* is the basal lineage and may have emerged earlier than the other clades, at least before the Asian Mid-Miocene radiations, c. 12.00–10.00 Mya which may have resulted in the diversification of the *R. chensinensis* polyphyletic clades (Fig. 4). This divergence resulted in the formation of a much younger clade, *R. kukunoris* (Early Pliocene; c. 5.0 Mya) with a well-developed toe webs as derivative character (Fig. 4).

3.2.4. Morphological crypticity

By matching the results of the morphological analysis with the cladistic scenarios, here the polyphyly and paraphyly of the *Rana* sourced from the trade, we provided evidence of clear morphological distinctions among the *Rana* originating from the trade for two variables only. The dorsal tubercles (also described as round dorsal glands) and the angle made by the webbing between the first and second toes (WTA) can be used to distinguish among the polyphyletic and parapatric clades, respectively (Fig. 5). This low level of morphological variation was especially prominent between *R. huanrenensis* and the member of the polyphyletic *R. chensinensis* clade (Figs. 5A and 5B). In addition, the morphology of *R. huanrenensis* was also very similar to that of the members of the parapatric clades: *R. uenoi* and *R. dybowskii* (Figs. 5A and 5C). The variance information for all 18 morphological variables extracted from polyphyletic *R. chensinensis*, *R. kukunoris* and *R. huanrenensis* (n = 89) discriminated round dorsal glands (PC2: 9.2%; Fig. 5B) as a key meristic trait to differentiate *R. kukunoris*. Whereas, the PCs extracted from the parapatric clades: *R. huanrenensis*, *R. uenoi* and *R. coreana* and *R. dybowskii* marked a significant distinction between the WTA of *R. coreana* (PC 2: 6.5%) and that of *R. dybowskii*, *R. huanrenensis* and *R. uenoi* (PC1: 83.5%), and supported by ANOVA and the Tukey test (Table S8).

3.2.5. Species assignment 3: comparative species delimitation coalescent methods

Here, we present the OTUs among the *Rana* originating from the trade (n = 171), estimated through the secondary species delimitation models using the coalescent-based method. This complements the primary species delimitation modelling with distance-based method performed in the previous section (refer to ABGD).

Species delimitation with the bPTP model delineated 22 OTUs within the *Rana* originating from the trade (n = 171; refer to bPTP partition; Fig. 5A) with the acceptance rate of 0.30. In details, bPTP model delimited two OTUs, representing *R. amurensis* (n = 1; PP = 1.0) and *R. coreana* (n = 4; PP = 0.897) in the monophyletic clade 1 (see tree in Fig. 5A). *Rana chensinensis* showed the signature of a nested clades (clade 5; Fig. 5A) with nine species boundaries that resulted in OTU 3 (n = 1, pp = 1.0; see bPTP partition in Fig. 5A), OTU 6 (n = 10; pp = 0.960; Fig. 5A), OTU 7 (n = 5; pp = 0.935; Fig. 5A), OTU 8 (n = 10; pp = 0.967; Fig. 5A), OTU 9 (n = 23; pp = 0.971; Fig. 5A), OTU 10 (n = 5; pp = 0.747; Fig. 5A), OTU 13 (n = 1; pp = 0.940; Fig. 5A), OTU 14 (n = 25; pp = 0.818; Fig. 5A) and OTU 15 (n = 13; pp = 0.605; Fig. 5A). The bPTP tree split *R. dybowskii* (Clade 3) into seven OTUs: OTU 4 (n = 3; pp = 0.981; Fig. 5A), OTU 11 (n = 5; pp = 0.947; Fig. 5A) OTU 12 (n = 7; pp = 0.622; Fig. 5A), OTU 17 (n = 3; pp = 0.515; Fig. 5A), and OTU 18 (n = 5; pp = 0.533; Fig. 5A). In addition, the bPTP model supported *R. kukunoris* as a single unit: OTU 5 (n = 13; pp = 0.767) in clade 5 (Fig. 5A). Finally, there were two OTUs delimited within *R. huanrenensis* (clade 4; Fig. 5A): OTU 19 (n = 7; PP = 0.811) and OTU 20 (n = 20; pp = 0.745), and another two within *R. dybowskii* (Clade 2; Fig. 5A): OTU 21 (n = 2; pp = 0.413) and OTU 22 (n = 6; pp = 0.659).

For the sGMYC model, we searched for the most probable single threshold time, a criterion used by the modelling to delimit the OTUs based on the transitional point from Yule to coalescent process in the tree. Our calibrated sGMYC tree, predicted the threshold time to have occurred in Mid-Miocene (c. 11.56 Mya; Fig. 5A). As a result, the sGMYC model delimited five clades based on the divergence of the stem clade around the threshold time (n OTUs = 5; maximum likelihood of sGMYC model = 333.198; Fig. 5A). The five delimited OTUs were represented by OTU 1 (polyphyletic clade 1: *R. amurensis* and *R. coreana*; Fig. 5A), OTU 2 (monophyletic clade 2; *R. dybowskii*), and OTU 3 (monophyletic clade 3: *R. dybowskii*; Fig. 5A). OTU 4 represented the monophyletic clade 4 that contained *R. huanrenensis* and some individuals from *R. dybowskii* and *R. chensinensis*; Fig. 5A). The OTU 5 represented the nested monophyletic clades of *R. chensinensis* and *R. kukunoris* as a single unit (Fig. 5A).

Table 2

Bayes factor delimitation (BFD) model evaluating the support of OTUs determined by the comparative species assignments. Machine learning approach using BFD modelling determined that the best-supported number of OTUs among the operative modes such as primary sequence screening with BLAST, followed by species delimitations with distance- and coalescent-based methods. The higher the MLE value indicates the higher the model support. All Bayes factor calculations are made against the default taxonomy model of BLAST. Therefore, the highest positive BF values indicate the most-supported taxonomy model.

Species assignment method	Operative mode	Method conservatism	Number of Operational taxonomic unit (OTU)	Marginal likelihood estimation (MLE)	Bayes factor	Rank of model support
BLAST	Heuristic method (sequence homologous)	High	8	-1429.792	–	4
ABGD	Genetic distance and barcoding gap	Moderate	12	-681.817	1495.95	1
bPTP	Coalescent	Lowest	24	-769.843	1319.90	2
sGMYC	Coalescent	Highest	5	-1125.496	608.592	3

3.2.6. Evaluation of best-supported OTUs

We improved the accuracy of species identification for a single 16S rRNA gene barcode with the model-based selection for the best-supported OTUs among the ones determined by the species assignment methods based on DNA sequences (ABGD, BLAST, sGMYC and bPTP). Here, Bayes Factor Delimitation (BFD) modelling and path sampling method selected the best-fitted OTUs scheme from the ABGD model, and provided support to the 12 OTUs as indicated by the highest marginal likelihood estimates (MLE) and a positive bayes factor value (model ABGD; MLE: -681.817; Bayes factor against default model: 1495.95; Table 2; Fig. 6).

3.2.7. Widespread origins of samples sourced from the trade

Our employment of the best-supported OTUs scheme, predetermined with the BFD model in the phylogenetic reconstruction, demonstrated the widespread geographic origins of brown frogs sourced from the trade. This was possible as the 16S rRNA gene marker is widely used, and additional homologous sequences originating from varying geographical ranges are archived in public database such as Genbank (here we treat them as control sequences).

The Bayesian Inference (BI) tree inferred from the 16S rRNA gene sequences recovered three highly supported monophyletic clades (Clades I, II and III; Fig. 7A). The most basal was Clade I (Bayesian posterior probability (BPP) = 0.82; Fig. 7A) containing the monophyletic *R. amurensis* (Clade I, OTU 10; BPP = 1.0; Fig. 7A), including both samples originating from the trade and control samples from northern China and northeastern Mongolia. *Rana amurensis* shared a sister relationship with the monophyletic clade *R. coreana* (Clade I; OTU 9; BPP = 1.0; Fig. 7A), including both traded and control *R. coreana*. Clade II (BPP = 0.61; Fig. 7A) contained the monophyletic clades of traded and control samples *R. uenoii* from Korea (OTUs 8 and 9; BPP = 0.99 – 1.0; Fig. 7A), and the monophyletic clade of traded *R. dybowskii* (OTUs 11 and 12; BPP = 0.86 – 1.0; Fig. 7A), distributed in northern China and southeastern Russia. Clade III (BPP = 1.0; Fig. 7A) encompassed the polyphyletic *R. chensinensis* (Clade III; OTU I, 2 and 7; BPP = 0.76 – 1.0; Fig. 7A), with the following nested clades: the monophyletic *R. kukunoris* (Clade III; OTUs 3 and 4; BPP = 100%; Fig. 7A) and the monophyletic *R. huanrenensis* (Clade III; OTUs 5 and 6; BPP = 0.92 and 0.8; Fig. 7A). The polyphyletic clade III represented *Rana* distributed from the eastern Qinghai Tibetan Plateau (*R. kukunoris*), south-central China (*R. chensinensis*), the central Asian mainland and northeastern Asia (*R. chensinensis*), and from northern China to the Korean Peninsula (*R. huanrenensis*).

4. Discussion

Our meta-analysis on cross-study comparisons revealed variations in species assignment accuracy based on methods including morphometry, genetic distance and genetic coalescence to infer OTUs, and estimate the levels and patterns of crypticity. Despite the species delimitation with coalescence being generally more sensitive to detect cryptic clade (Table 1), we do not agree on saying that this method outperformed the less sensitive ones. ABGD distance based and morphometry are also informative to infer different levels of crypticity (Fig. 1).

As an improvement to the insufficient workflows involving barcoding and species delimitation analyses as a first approach to taxonomic assignments of alien species, the integrative workflow we propose here also includes morphometry and phylogenetic traits (Figs. 3 and 4) and a model-based OTUs phylogeny (Fig. 7). Defining the modelling variables for the OTUs to determine the best-supported model before the analyses (Fig. 6) is especially crucial to help tracing the origins of cryptic species (Fig. 7). This practice is, however, infrequently conducted by modern taxonomists as most studies rely on the uniformity of results originating from different

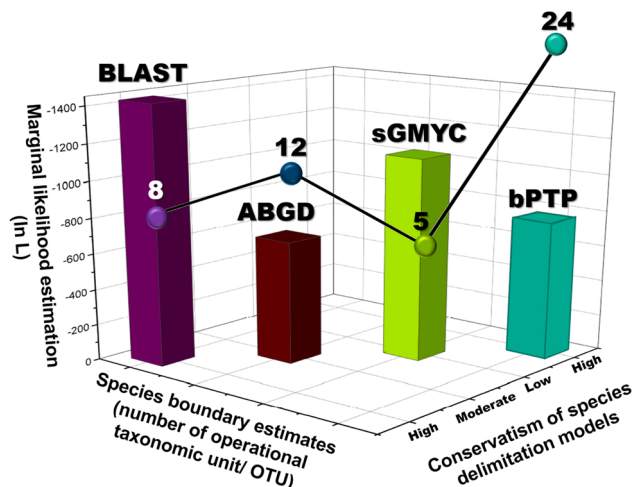


Fig. 6. Best-supported operational taxonomic units (OTUs) among the *Rana* brown frog originated from trade. (A) The schemes represent four different species assignment methods using DNA sequences (BLAST, ABGD, sGMYC and bPTP) for a single locus of barcode 16S rRNA. The support for each species model was determined with the Bayes factor delimitation (BFD). The bar charts indicate the likelihood values of MLE support. The ABGD method (OTUs = 12) is best most-supported. The line graph indicates the number of OTUs estimated by each scheme.

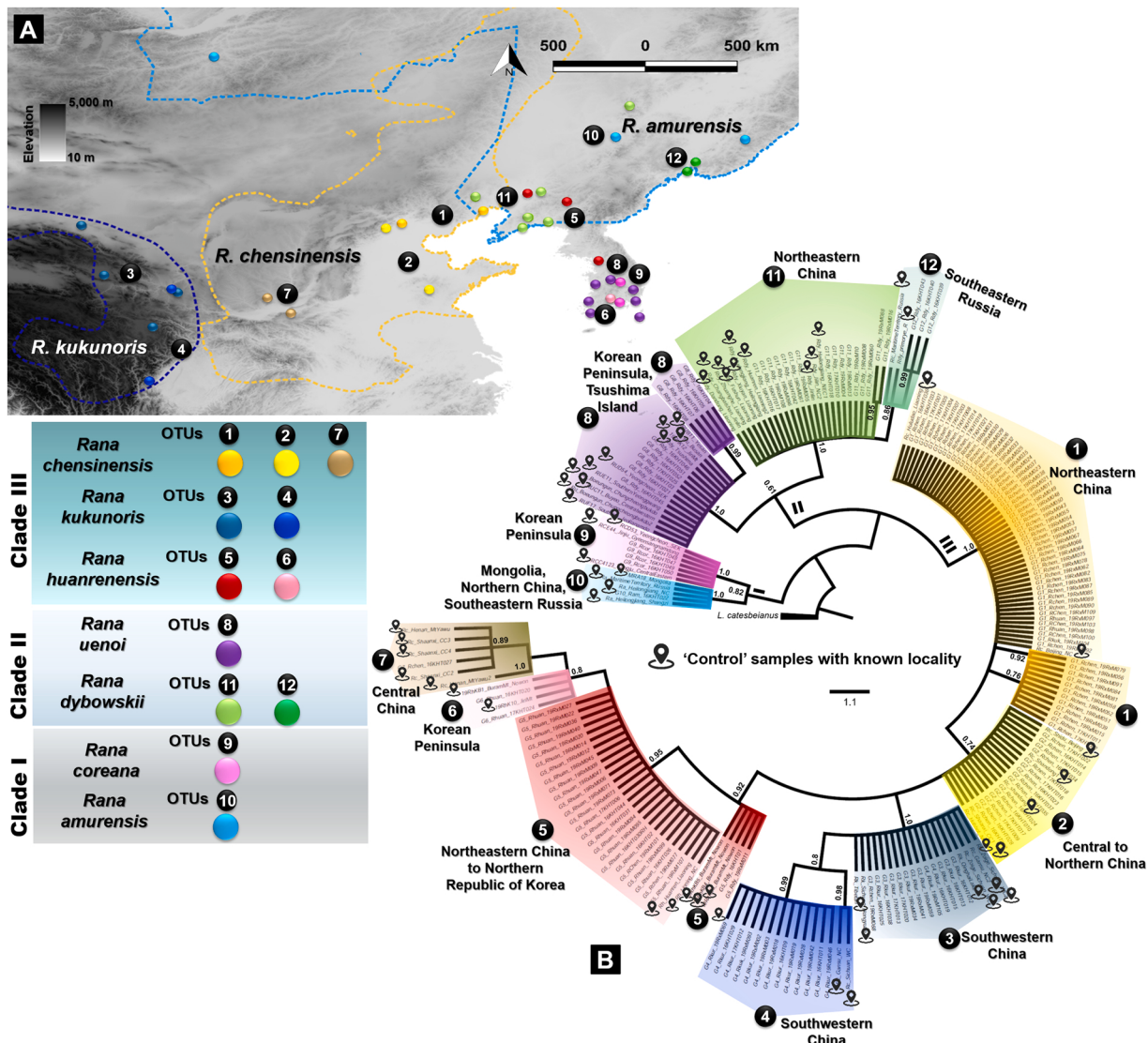


Fig. 7. Origin of brown frog *Rana* traded into the Republic of Korea using a model-based OTUs and phylogeny. (A) The Bayesian Inference (BI) tree supports the widespread origin of traded *Rana* across northeast China, with the likely origins for each OTU marked on the map. (B) Bayesian Inference (BI) tree reconstructed from 202 assembled 16S rRNA barcode sequences of traded brown frogs (between 2016 and 2019) and control sequences from Genbank (Table S2 for sample list). The species and OTUs are colour coded and matching the colours of the tree nodes. The number for each clade indicates the number of OTU and the control specimens with known locality are marked at the nodes of tree. For visual representation, species names are abbreviated as *R. chensinensis* (Rch), *R. dybowskii* (Rd), *R. kukunoris* (Rk), *R. huanrenensis* (Rh), *R. coreana* (Rco) and *R. uenoi* (Ru).

methods (forest plots; Figs. S1-S6), a challenging task to achieve with potentially incorrect taxonomic implications. We highlight that unifying the species assignment methods (refer to the graphical abstract) improves the ability to rely on common barcoding, such as 16S rRNA gene fragment, and potentially other universal single barcoding marker. In our case, the 16S rRNA gene barcode helped inferring the varying levels of crypticity in the *Rana* traded between People's Republic of China (hereafter China) and the Republic of Korea.

In our case study, the BFD modelling based on the different OTUs information models provided support for a moderately conservative model of ABGD (12 OTUs; Fig. 5A), indicating a reasonable level of crypticity in the ESU among the *Rana* sourced from the trade (Fig. 7B). However, an increase in the size of ESUs (Mohanty and Measey, 2019) reduces the accuracy of conservation units (Kats and Ferrer, 2003). Similarly, the *Rana* sourced from the trade are phenotypically and genetically cryptic, resulting in a large number of cryptic OTUs delimited by the bPTP scheme (second best-fitted OTUs scheme; Table 1; Fig. 6) in comparison to the number of described species ($n = 6$; Fig. 2A). Therefore, the risk of blurring ESUs through introduction and hybridisation is high, and we can expect the size of the ESUs to fluctuate if the release of traded individuals continues.

4.1. Frogs harvest and trade

There are currently three species in the genus recognized in the Republic of Korea: *R. uenoii*, *R. coreana*, and *R. huanrenensis*. However, the importation of *Rana* into the country for food market is erroneous, as the imported species are labelled under the same names as the native species (mostly *R. uenoii*), but the actual identity of the imported individuals are largely unchecked remain dubious due to the lack of consistent identification framework. In addition, surplus animals from the trade are regularly released into the wild at the end of each trading season, and frog dealers are completely unaware of invasive potential of these frogs. This situation, therefore, presents potential breaches in biosecurity and opportunities for cryptic invasion of non-native species.

In this study we demonstrate the mismanagement in the international trade of brown frogs, resulting from the likely wild-harvested frog species native to China: *R. kukunoris* and *R. chensinensis*. We showed the phenotypic and genetic crypticity between the imported *R. chensinensis* and the native Korean frog *R. huanrenensis* in the Republic of Korea, highlighting the detrimental impacts of current frog trades between the Republic of Korea and China.

The *Rana* individuals sourced for the trade were not the farm-bred *R. dybowskii* or *R. uenoii* as advertised (Fig. 7A). Farming would involve several generations, and as these individuals are not *R. dybowskii*, hybridisation with other species would be detectable, but the clear species boundaries highlight that it is not the case (Fig. 7B), and point further towards the harvesting of frogs from the wild. While it is not possible to clarify if they were wild-caught or the species are erroneously farmed because of the cryptic morphological characters, clearly, a natural range expansion is not a question here as we provide evidence of widespread origins across East Asia for three species (*R. kukunoris*, *R. chensinensis* and *R. amurensis*; Fig. 7A). Through model-based OTUs phylogeny, we traced the harvesting localities of brown frogs and potential transportation routes for the trade within China, and provide evidences about the mismanagement in imports and trade practices between China and the Republic of Korea. For instance, *R. kukunoris* is restricted to the mountainous landscapes of the eastern Qinghai Tibetan Plateau, and the frogs must have been transported from farms, or wild harvests, in western China towards the northeast of the country before being exported towards the Republic of Korea. Although some species of farmed frogs are legally traded following authorizations from the government, a popular method is semi-farming *Rana* species. This is an alternative to wild harvests, but semi-farming is a non-selective procedure that may result in the capture of non-focal species, and potentially contributes to their declines. Illegal harvests and transportation may also exist, driven by the unbalance demands, and therefore exacerbating the risk of population declines. This issue is alarming as wildlife harvests are among the top contributors of amphibian population declines (Regehr et al., 2017), and proper management must be implemented. Additionally, we demonstrate that *R. uenoii* are likely wild caught in Korea and added to the stock for monetary benefits (see OTU 8 in Clade II; Fig. 7A).

The single *R. amurensis* individual raises some question, and it is likely a random individual that went unnoticed by the traders (Fig. 2). This again points at the fact that individuals are not farmed, as a single individual from a different species cannot maintain the species identity while admixing with other congeneric species in a farm setting. This individual also indicates a lack of knowledge and education on the proper identification of traded animals by the exporters, customs officers, and importers, allowing for the illegal trade masked by the “legal trade” in view of the Korean law. We recognise the difficulties of identifying cryptic species, but the education of customs officers and agencies in charge of regulating the animal trade in both countries is required, regarding the threats resulting from the amphibian trade, and especially biological threats such as invasion and disease transmission. Adequate awareness would at least prevent the sellers from releasing unsold individuals to the wild, as sellers do follow “welfare practices” and release unsold frogs at the end of the sales period to avoid the unnecessarily killing of frogs.

4.2. Ecological impact of the amphibian trade

The international trade involves wild-caught *Rana* individuals must be controlled as currently much more than what is ‘legal’ is crossing the border (between China and Korea). While all traded individuals are meant to originate from Jilin province where farming of *R. chensinensis* is legal for instance, the species is not occurring there. Our results pinpoint the widespread origin across central and northeastern China for the *Rana* traded towards Korea, and specifically for the OTUs delineated by the clades *R. chensinensis* and *R. kukunoris* (clade III; Fig. 7). A necessity for further study to explore the crypticity in the focal clades is warranted, similarly to the urgent need to identify and taxonomically describe the geographically isolated OTUs within the *R. kukunoris* clade on the eastern Qinghai-Tibetan Plateau (see distribution of clade III; Fig. 7), and treat them as segregated conservation units.

The illegal importation of *R. amurensis*, *R. chensinensis* and *R. kukunoris* (Fig. 2) to the Republic of Korea is threatening biodiversity for several reasons, and most notably the risks of invasion and disease transmission. While the farming and trade *R. huanrenensis* is legal in the Republic of Korea, it is also threatening local populations because of the presence of different and importantly divergent allopatric OTUs, and therefore, conservation units in the two countries. The OTU 5 within the *R. huanrenensis* clade is not native to the Republic of Korea (Fig. 7), and while its consumption would not impact the ecology of the local species, the risk of escape and establishment of populations in the wild is extremely likely (Borzée et al., 2021a). The inadvertent introduction could result in hybridisation and the loss of the unique population structure and local adaptation of Korean *R. huanrenensis*. Similarly, the over-exploitation of Giant salamanders (*Andrias* sp.) for foods and trade resulted in the five species merging into one hybrid swarm, and some lineages at the species level are now lost due to the unnatural hybridisation (Yan et al., 2018), also impacting the fitness and adaptation to the local environment (Crawford et al., 2013).

Extra attention should be brought to the legitimacy of importing *R. huanrenensis* for consumption. Our results showed that native Korean *R. huanrenensis* was the most susceptible species from the impact of the amphibian trade due to the high phenotypic and genetic crypticity with the non-native polyphyletic *R. chensinensis* and *R. kukunoris* (Fig. 5C).

The case of *R. dybowskii* is a bit different. While the trade of this species should now be illegal as the species is not native to the

Republic of Korea, *R. uenoi* was split from *R. dybowskii* only recently (Yang et al., 2017; Jeon et al., 2021), succeeding years after the country allowed commercial frog farming since 2005 and permitted the international import of brown frogs species already natively present in the country (Kim et al., 2016). However, it took until 2017 for the Ministry of Environment of the Republic of Korea to officially recognise the dichotomy between *R. dybowskii* and *R. uenoi* (Yang et al., 2017). Although the natural range justified the former legality of the trade of *R. dybowskii*, from the genetic standpoint the trade could only have detrimental effect on the Korean populations (Song et al., 2006; Yang et al., 2017). The late recognition of *R. uenoi* by the Ministry of Environment in the Republic of Korea may have had a price on the native species, as the presence of invasive populations needs to be investigated. In addition, trade to other nations should also be halted. *Rana dybowskii* ranges into the Democratic People's Republic of Korea with unknown southern range boundaries, and similarly *R. uenoi* ranges at least as far north as Pyongyang (Borzée et al., 2021b). The trade of *R. dybowskii* anywhere within that range should therefore be stopped. Similarly, other amphibian species are illegally traded towards the Republic of Korea, generally through the pet trade (Koo et al., 2020) and pet-releases are not uncommon (Borzée et al., 2021a), so the risks posed by introduction and establishment of potentially invasive amphibians should be addressed urgently.

4.3. Potential morphometric traits key for species identification

Despite the indefinite variations in brown frogs phenotypic, the toe webbings show a clear morphological divergences and are adequate as a general morphometric key for species assignment. The angle made by the webbing between the first and the second toes (WTA) and the presence of round dorsal glands are the two key morphological traits effective to identify *Rana* species, and therefore a tool to monitor the trade. While the presence of tubercles is a highly visible meristic trait (Table S1), WTA is less obvious to the untrained eye, but it is species-specific in northeastern Asian *Rana* (Fig. 4). The distribution of WTA across the northeastern Asian *Rana* lineage suggests that the ancestral character is the closest to that of *R. coreana* (Fig. 4). The structure of toe webbing in *R. coreana* is well-developed, but underexposed and forming an acute angle (Song et al., 2006), while a better characterized toe webbings derived from the ancestral state evolved in *R. kukunoris* (Fig. 4). This distinction is presumably driven by adaptation to specific habitats as the species is restricted to the high altitudes of the eastern Qinghai Tibetan Plateau (Leung et al., 2021), where adaptation is likely associated with locomotion (Zhou et al., 2012). Within species occurring in China, the head length and the distance between the eyes are important traits for identification (Fig. 3), and they can be used to identify the species in *Rana* farms. A development of key meristic and morphometric traits as a quick identification guideline is recommendable practice for farms, and especially when individuals are eventually to be traded outside of the range of their native OTUs.

5. Conclusions

In the first section of this study, the meta-analysis helped reveal the variations in the sensitivity or efficiency of common analytical methods used for species assignments: morphometry, barcoding with genetic distances and species delimitation with coalescence, in inferring potential operational taxonomical units (OTUs). The differences in sensitivity amongst the comparative analytical methods do not affect the reliability of any of the methods as each of them is informative about the different levels of crypticity. The second section highlighted our integrative workflow using morphometry, single locus barcoding, OTU-based phylogeny and species delimitation modelling as adequate and practical for the first attempt at identifying unknown, trade-sourced amphibian specimens, such as cryptic northeast Asian brown frogs. Our study also demonstrates the mismanagement in the frog trade and the likely harvest of wild frogs among the species traded from China: *R. kukunoris* and *R. chensinensis*. We provided support on the phenotypic and genetic crypticity between the imported *R. chensinensis* and the native Korean frog *R. huanrenensis*, highlighting the risks linked to the current frog trade in northeast Asia. Despite the lack of distinctive morphological traits to distinguish the northeast Asian brown frogs' phenotypes, the structure of toe webbing showed morphological divergence between species and it can be reasonably acceptable as the key identification trait for species identification, despite requiring tools to measure the angles. Therefore, we suggested its use as a general key morphometric trait supporting the highly visible meristic trait(s) that help lower the number of potential species identities, noting that not all species display such a trait.

Declaration of Competing Interest

The authors declare that they have no known competing financial interests or personal relationships that could have appeared to influence the work reported in this paper.

Data availability

All DNA sequences isolated in this study were deposited to Genbank (<https://www.ncbi.nlm.nih.gov/nuccore>) under the accession numbers: MZ349886–MZ519854 .

Acknowledgements

The authors thank Hyunjung Kim for providing a photo for Fig. 5. The manuscript benefitted from reconstructive comments from Dr. Mi-Sook Min (Professor, Seoul National University, Republic of Korea). This project was financially supported by Korea Environmental Industry and Technology Institute (KEITI) of Republic of Korea under a project entitled 'Development of behavioural

ecological methods for population regulation of invasive amphibians and reptiles' (Step 2) with grant number KEITI 2021002270001 to YJ, and the Foreign Youth Talent Program (QN2021014013L) from the Ministry of Science and Technology of the People's Republic of China to AB.

CRediT authorship contribution statement

SNO and AB conceived and designed the analysis. YS, HTK, MFC, YB and AB collected the data. YJ and ZY verified the data and supported the conceptual framework of the project. SNO performed the analysis, and YS, MFC and JH contributed to the data analysis tools. SNO wrote the manuscript and AB helped the interpretation of data. All authors involved in the editing of manuscript.

Data and code availability

All DNA sequences isolated in this study were deposited to Genbank (<https://www.ncbi.nlm.nih.gov/nuccore>) under the accession numbers: MZ349886-MZ519854 (16S rRNA gene sequences; see [Table S2 in supplemental information](#)). List of references used for reviewing the sensitivity of species assignment methods and all original codes, xml inputs and coding data generated during the analyses are available in following public database Othman, S. N. (2022) "Evaluating the efficiency of popular species identification analytical methods, and integrative workflow using morphometry and barcoding bioinformatics for taxonomy and origin of traded cryptic brown frogs", Mendeley Data, V2, doi:10.17632/mtd4yszp3d.2, <https://data.mendeley.com/datasets/mtd4yszp3d/2>. Any additional information required to reanalyse the data reported in this paper is available from the corresponding author upon request.

Appendix A. Supporting information

Supplementary data associated with this article can be found in the online version at [doi:10.1016/j.gecco.2022.e02253](https://doi.org/10.1016/j.gecco.2022.e02253).

References

- Altschul, S.F., Gish, W., Miller, W., Myers, E.W., Lipman, D.J., 1990. Basic local alignment search tool. *J. Mol. Biol.* 215, 403–410. [https://doi.org/10.1016/S0022-2836\(05\)80360-2](https://doi.org/10.1016/S0022-2836(05)80360-2).
- Auliya, M., Altherr, S., Ariano-Sanchez, D., Baard, E.H., Brown, C., Brown, R.M., Cantu, J.C., Gentile, G., Gildenhuys, P., Henningheim, E., Hintzmann, J., Kanari, K., Kravac, M., Lettink, M., Lippert, J., Luiselli, L., Nilson, G., Nguyen, T.Q., Nijman, V., Parham, J.F., Pasachnik, S.A., Pedrono, M., Rauhaus, A., Córdova, D.R., Sanchez, M.E., Schepp, U., van Schingen, M., Schneeweiss, N., Segniagbeto, G.H., Somaweera, R., Sy, E.Y., Türkozan, O., Vinke, S., Vinke, T., Vyas, R., Williamson, S., Ziegler, T., 2016a. Trade in live reptiles, its impact on wild populations, and the role of the European market. *Biol. Conserv.* 204, 103–119. <https://doi.org/10.1016/j.biocon.2016.05.017>.
- Auliya, M., García-Moreno, J., Schmidt, B.R., Schmeller, D.S., Hoogmoed, M.S., Fisher, M.C., Pasmans, F., Henle, K., Bickford, D., Martel, A., 2016b. The global amphibian trade flows through Europe: the need for enforcing and improving legislation. *Biodivers. Conserv.* 25, 2581–2595. <https://doi.org/10.1007/s10531-016-1193-8>.
- Baele, G., Lemey, P., Vansteelandt, S., 2013. Make the most of your samples: Bayes factor estimators for high-dimensional models of sequence evolution. *BMC Bioinforma.* 14, 1–18. <https://doi.org/10.1186/1471-2105-14-85>.
- Birch, J.L., Walsh, N.G., Cantrill, D.J., Holmes, G.D., Murphy, D.J., 2017. Testing efficacy of distance and tree-based methods for DNA barcoding of grasses (Poaceae tribe Poeae) in Australia. *PLoS ONE* 12, e0186259.
- Blackburn, T.M., Pysek, P., Bacher, S., Carlton, J.T., Duncan, R.P., Jarošký, V., Wilson, J.R.U., Richardson, D.M., 2011. A proposed unified framework for biological invasions. *Trends Ecol. Evol.* 26, 333–339. <https://doi.org/10.1016/j.tree.2011.03.023>.
- Borkent, A., 2021. Diagnosing diagnoses – can we improve our taxonomy? *ZooKeys* 1071, 43–48. <https://doi.org/10.3897/zookeys.1071.72904>.
- Borzée, A., Kwon, S., Koo, K.S., Jang, Y., 2020a. Policy recommendation on the restriction on amphibian trade toward the Republic of Korea. *Front. Environ. Sci.* 8, 129. <https://doi.org/10.3389/fenvs.2020.00129>.
- Borzée, A., McNeely, J., Magellan, K., Miller, J.R.B., Porter, L., Dutta, T., Kadinjappalli, K.P., Sharma, S., Shahabuddin, G., Aprilinayati, F., Ryan, G.E., Hughes, A., Abd Mutualib, A.H., Wahab, A.Z.A., Bista, D., Chavanich, S.A., Chong, J.L., Gale, G.A., Ghaffari, H., Ghimirey, Y., Jayaraj, V.K., Khatiwada, A.P., Khatiwada, M., Krishna, M., Lwin, N., Paudel, P.K., Sadykova, C., Savini, T., Shrestha, B.B., Strine, C.T., Sutthacheep, M., Wong, E.P., Yeemin, T., Zahirudin, N.Z., Zhang, L., 2020b. COVID-19 highlights the need for more effective wildlife trade legislation. *Trends Ecol. Evol.* 35, 5–8. <https://doi.org/10.1016/j.tree.2020.10.001>.
- Borzée, A., Kielgast, J., Wren, S., Angulo, A., Chen, S., Magellan, K., Messenger, K.R., Hansen-Hendrikx, C.M., Baker, A., Santos, M.M.D., Kusrini, M., Jiang, J., Maslova, I.V., Das, I., Park, D., Bickford, D., Murphy, R.W., Che, J., Van Do, T., Nguyen, T.Q., Chuang, M.F., Bishop, P.J., 2021a. Using the 2020 global pandemic as a springboard to highlight the need for amphibian conservation in eastern Asia. *Biol. Conserv.* 255, 108973 <https://doi.org/10.1016/j.biocon.2021.108973>.
- Borzée, A., Litvinchuk, S.N., Ri, K., Andersen, D., Nam, T.Y., Jon, G.H., Man, H.S., Choe, J.S., Kwon, S., Othman, S.N., Messenger, K., Bae, Y., Shin, Y., Kim, A., Maslova, I., Luedtke, J., Hobin, L., Moores, N., Seliger, B., Glenk, F., Jang, Y., 2021b. Update on distribution and conservation status of amphibians in the democratic people's republic of Korea: conclusions based on field surveys, environmental modelling, molecular analyses and call properties. *Animals* 11, 2057. <https://doi.org/10.3390/ani11072057>.
- Bouckaert, R., Heled, J., Kühnert, D., Vaughan, T., Wu, C.H., Xie, D., Suchard, M.A., Rambaut, A., Drummond, A.J., 2014. BEAST 2: a software platform for bayesian evolutionary analysis. *PLoS Comput. Biol.* 10, 1–6. <https://doi.org/10.1371/journal.pcbi.1003537>.
- Bouckaert, R., Vaughan, T.G., Barido-Sottani, J., Duchêne, S., Fourment, M., Gavryushkina, A., Heled, J., Jones, G., Kühnert, D., De Maio, N., Matschiner, M., Mendes, F.K., Müller, N.F., Ogilvie, H.A., du Plessis, L., Popinga, A., Rambaut, A., Rasmussen, D., Siveroni, I., Suchard, M.A., Wu, C.H., Xie, D., Zhang, C., Stadler, T., Drummond, A.J., 2019. BEAST 2.5: An advanced software platform for Bayesian evolutionary analysis. *PLoS Comput. Biol.* 15, e1006650 <https://doi.org/10.1371/journal.pcbi.1006650>.
- Bull, J.J., 1987. Evolution of phenotypic variance. *Evolution* 41, 303. <https://doi.org/10.2307/2409140>.
- Camargo, A., Morando, M., Avila, L.J., Sites, J.W., 2012. Species delimitation with abc and other coalescent-based methods: A test of accuracy with simulations and an empirical example with lizards of the *Liolaemus darwini* complex (Squamata: Liolaemidae). *Evolution* 66, 2834–2849. <https://doi.org/10.1111/j.1558-5646.2012.01640.x>.
- Čandek, K., Kuntner, M., 2014. DNA barcoding gap: reliable species identification over morphological and geographical scales. *Mol. Ecol. Resour.* 15, 268–277. <https://doi.org/10.1111/1755-0998.12304>.

- Chan, K.O., Grismer, L.L., 2019. To split or not to split? Multilocus phylogeny and molecular species delimitation of southeast Asian toads (family: Bufonidae). *BMC Evolut. Biol.* 19, 95. <https://doi.org/10.1186/s12862-019-1422-3>.
- Cohen, J., 1988. *Statistical Power Analysis for the Behavioral Sciences*, Second edi. ed.... Lawrence Erlbaum Associates,, New York.
- Correa, C., Vásquez, D., Castro-Carrasco, C., Zúñiga-Reinoso, Á., Ortiz, J.C., Palma, R.E., 2017. Species delimitation in frogs from South American temperate forests: the case of *Eupsophus*, a taxonomically complex genus with high phenotypic variation. *PLoS ONE* 12, 1–21. <https://doi.org/10.1371/journal.pone.0181026>.
- Crawford, A.J., Cruz, C., Griffith, E., Ross, H., Ibáñez, R., Lips, K.R., Driskell, A.C., Bermingham, E., Crump, P., 2013. DNA barcoding applied to ex situ tropical amphibian conservation programme reveals cryptic diversity in captive populations. *Mol. Ecol. Resour.* 13, 1005–1018. <https://doi.org/10.1111/1755-0998.12054>.
- Darriba, D., Taboada, G.L., Doallo, R., Posada, D., 2015. jModelTest 2: more models, new heuristics and high- performance computing. *Eur. PMC Funders Group* 9, 6–9. <https://doi.org/10.1038/nmeth.2109.jModelTest>.
- Dong, B., Zhou, Y., Yang, B., 2016. The complete mitochondrial genome of the *Rana huanrenensis* (Anura: Ranidae). *Mitochondrial DNA Part A: DNA Mapp., Seq., Anal.* 27, 4551–4552. <https://doi.org/10.3109/19401736.2015.1101558>.
- Faulkner, K.T., Robertson, M.P., Wilson, J.R.U., 2020. Stronger regional biosecurity is essential to prevent hundreds of harmful biological invasions. *Glob. Change Biol.* 26, 2449–2462. <https://doi.org/10.1111/gcb.15006>.
- Firkowski, C.R., Bornschein, M.R., Ribeiro, L.F., Pie, M.R., 2016. Species delimitation, phylogeny and evolutionary demography of co-distributed, montane frogs in the southern Brazilian Atlantic Forest. *Mol. Phylogenetics Evol.* 100, 345–360. <https://doi.org/10.1016/j.ympev.2016.04.023>.
- Fourdrilis, S., Backeljau, T., 2019. Highly polymorphic mitochondrial DNA and deceiving haplotypic differentiation: Implications for assessing population genetic differentiation and connectivity. *BMC Evolut. Biol.* 19, 1–16. <https://doi.org/10.1186/s12862-019-1414-3>.
- Fujisawa, T., Barracough, T.G., 2013. Delimiting species using single-locus data and the generalized mixed yule coalescent approach: A revised method and evaluation on simulated data sets. *Syst. Biol.* 62, 707–724. <https://doi.org/10.1093/sysbio/syt033>.
- García-Díaz, P., Ross, J.V., Woolnough, A.P., Cassey, P., 2017. The illegal wildlife trade is a likely source of alien species. *Conserv. Lett.* 10, 690–698. <https://doi.org/10.1111/conl.12301>.
- Gaytán, Á., Bergsten, J., Canelo, T., Pérez-Izquierdo, C., Santoro, M., Bonal, R., 2020. DNA Barcoding and geographical scale effect: the problems of undersampling genetic diversity hotspots. *Ecol. Evol.* 10, 10754–10772. <https://doi.org/10.1002/ece3.6733>.
- Groffen, J., Kong, S., Jang, Y., Borzée, A., 2019. The invasive american bullfrog (*Lithobates catesbeianus*) in the republic of korea: history and recommendations for population control. *Manag. Biol. Invasions* 10, 517–535. <https://doi.org/10.3391/mbi.2019.10.3.08>.
- Grummer, J.A., Bryson, R.W., Reeder, T.W., 2014. Species delimitation using bayes factors: simulations and application to the *Sceloporus scalaris* species group (Squamata: Phrynosomatidae). *Syst. Biol.* 63, 119–133. <https://doi.org/10.1093/sysbio/syt069>.
- Horvitz, N., Wang, R., Wan, F.H., Nathan, R., 2017. Pervasive human-mediated large-scale invasion: analysis of spread patterns and their underlying mechanisms in 17 of China's worst invasive plants. *J. Ecol.* 105, 85–94. <https://doi.org/10.1111/1365-2745.12692>.
- Huelsenbeck, J.P., Ronquist, F., 2001. MRBAYES: Bayesian inference of phylogenetic trees. *Bioinformatics* 17, 754–755. <https://doi.org/10.1093/bioinformatics/17.8.754>.
- Hughes, A.C., Marshall, B.M., Strine, C., 2021. Gaps in global wildlife trade monitoring leave amphibians vulnerable. *eLife* 10, e70086. <https://doi.org/10.7554/elife.70086>.
- Hulme, P.E., 2009. Trade, transport and trouble: managing invasive species pathways in an era of globalization. *J. Appl. Ecol.* 46, 10–18. <https://doi.org/10.1111/j.1365-2664.2008.01600.x>.
- Jarić, I., Heger, T., Castro Monzon, F., Jeschke, J.M., Kowarik, I., McConkey, K.R., Pyšek, P., Sagouis, A., Essl, F., 2019. Crypticity in biological invasions. *Trends Ecol. Evol.* 34, 291–302. <https://doi.org/10.1016/j.tree.2018.12.008>.
- Jeon, J.Y., Cho, S., Suk, H.Y., Lee, C.H., Ra, N.Y., Borzée, A., Song, J.H., Lee, H., Min, M.S., 2021. Resolving the taxonomic equivocacy and the population genetic structure of *Rana uenoi*. *Salamandrina* in press.
- Jeong, T.J., Jun, J., Han, S., Kim, H.T., Oh, K., Kwak, M., 2013. DNA barcode reference data for the Korean herpetofauna and their applications. *Mol. Ecol. Resour.* 13, 1019–1032. <https://doi.org/10.1111/1755-0998.12055>.
- Jörger, K.M., Norenburg, J.L., Wilson, N.G., Schrödl, M., 2012. Barcoding against a paradox? Combined molecular species delineations reveal multiple cryptic lineages in elusive meiofaunal sea slugs. *BMC Evolut. Biol.* 12, 245. <https://doi.org/10.1186/1471-2148-12-245>.
- Josse, J., Husson, F., 2016. missMDA: A package for handling missing values in multivariate data analysis. *J. Stat. Softw.* 70, 1–30. <https://doi.org/10.18637/jss.v070.i01>.
- Kats, L.B., Ferrer, R.P., 2003. Alien predators and amphibian declines: Review of two decades of science and the transition to conservation. *Divers. Distrib.* 9, 99–110. <https://doi.org/10.1046/j.1472-4642.2003.00013.x>.
- Kil, J., Kim, C.-G., 2014. Overview of preventive measures against invasive alien species in Korea and suggestions for their improvement. *Korean J. Ecol. Environ.* 47, 239–246. <https://doi.org/10.11614/ksl.2014.47.4.239>.
- Kim, J., Koo, K., Park, J., Kwon, S., Choia, W., Cho, H., Park, D., 2016. The first report on the Acanthocephalan infection of the Dybowskii's Brown Frogs (*Rana dybowskii*) collected inside and outside the commercial frog farms in Korea. *Korean J. Environ. Ecol.* 30, 694–704.
- Kim, J.B., Min, M.S., Yang, S.Y., Matsui, M., 2002. Genetic relationships among Korean brown frog species (Anura, Ranidae), with special reference to evolutionary divergences between two allied species *Rana dybowskii* and *R. huanrenensis*. *Zool. Sci.* 19, 369–382. <https://doi.org/10.2108/zsj.19.369>.
- Kimura, M., 1980. Evolutionary rates models. *J. Mol. Evol.* 16, 111–120. <https://doi.org/10.1007/BF01731581>.
- Koo, K.S., Park, H.R., Choi, J.H., Sung, H.C., 2020. Present status of non-native amphibians and reptiles traded in Korean online pet shop. *Korean J. Environ. Ecol.* 34, 106–114.
- Kosmala, G., Christian, K., Brown, G., Shine, R., 2017. Locomotor performance of cane toads differs between native-range and invasive populations. *R. Soc. Open Sci.* 4. <https://doi.org/10.1098/rsos.170517>.
- Kostov, B., Bécue-Bertaut, M., Husson, F., 2013. Multiple factor analysis for contingency tables in the FactoMineR package. *R. J.* 5, 29–38. <https://doi.org/10.32614/rj.2013-003>.
- Laking, A.E., Ngo, H.N., Pasmans, F., Martel, A., Nguyen, T.T., 2017. *Batrachochytrium salamandrivorans* is the predominant chytrid fungus in Vietnamese salamanders. *Sci. Rep.* 7, 44443. <https://doi.org/10.1038/srep44443>.
- Lanfear, R., Frandsen, P.B., Wright, A.M., Senfeld, T., Calcott, B., 2017. Partitionfinder 2: New methods for selecting partitioned models of evolution for molecular and morphological phylogenetic analyses. *Mol. Biol. Evol.* 34, 772–773. <https://doi.org/10.1093/molbev/msw260>.
- Leung, K.W., Yang, S., Wang, X., Tang, K., Hu, J., 2021. Ecogeographical adaptation revisited: morphological variations in the plateau brown frog along an elevation gradient on the Qinghai-Tibetan Plateau. *Biology* 10. <https://doi.org/10.3390/biology10111081>.
- Li, J., Yin, W., Xia, R., Lei, G., Fu, C., 2016. Complete mitochondrial genome of a brown frog, *Rana kunyuensis* (Anura: Ranidae). *Mitochondrial DNA* 27, 34–35. <https://doi.org/10.3109/19401736.2013.869681>.
- Marshall, B.M., Strine, C., Hughes, A.C., 2020. Thousands of reptile species threatened by under-regulated global trade. *Nat. Commun.* 11, 4738. <https://doi.org/10.1038/s41467-020-18523-4>.
- Mason, N.A., Fletcher, N.K., Gill, B.A., Funk, W.C., Zamudio, K.R., 2020. Coalescent-based species delimitation is sensitive to geographic sampling and isolation by distance. *Syst. Biodivers.* 18, 269–280. <https://doi.org/10.1080/14772000.2020.1730475>.
- Matsui, M., 2014. Description of a New Brown Frog from Tsushima Island, Japan (Anura: Ranidae: *Rana*). *Zool. Sci.* 31, 613–620. <https://doi.org/10.2108/zsj.140080>.
- Mohanty, N.P., Measey, J., 2019. The global pet trade in amphibians: species traits, taxonomic bias, and future directions. *Biodivers. Conserv.* 28, 3915–3923. <https://doi.org/10.1007/s10531-019-01857-x>.
- Morais, P., Reichard, M., 2018. Cryptic invasions: A review. *Sci. Total Environ.* 613–614, 1438–1448. <https://doi.org/10.1016/j.scitotenv.2017.06.133>.
- Morton, O., Scheffers, B.R., Haugaaen, T., Edwards, D.P., 2021. Impacts of wildlife trade on terrestrial biodiversity. *Nat. Ecol. Evol.* 5, 540–548. <https://doi.org/10.1038/s41559-021-01399-y>.

- Mun, S., Nam, K., Kim, C., Chun, Y.J., Lee, H.W., Kil, J.H., Lee, J.C., 2013. Suggestions for the improvement of the invasive alien species management in Korea - A comparative analysis of the legal framework for invasive alien species between Japan and Korea. *J. Environ. Policy Adm.* 21, 35–54.
- Nei, M., 1972. Genetic Distance between Populations. *Am. Nat.* 106, 283–292.
- Nguyen, N., Warnow, T., Pop, M., White, B., 2016. A perspective on 16S rRNA operational taxonomic unit clustering using sequence similarity. *npj Biofilms Micro* 2, 16004. <https://doi.org/10.1038/npjbiofilms.2016.4>.
- Nijman, V., Shepherd, C.R., 2011. The role of Thailand in the international trade in CITES-listed live reptiles and amphibians. *PLoS ONE* 6, 1–7. <https://doi.org/10.1371/journal.pone.0017825>.
- O'Hanlon, S.J., Rieux, A., Farrer, R.A., Rosa, G.M., Waldman, B., Bataille, A., Kosch, T.A., Murray, K.A., Brankovics, B., Fumagalli, M., Martin, M.D., Wales, N., Alvarado-Rybäk, M., Bates, K.A., Berger, L., Böll, S., Brookes, L., Clare, F., Courtois, E.A., Cunningham, A.A., Doherty-Bone, T.M., Ghosh, P., Gower, D.J., Hintz, W.E., Höglund, J., Jenkinsen, T.S., Lin, C.F., Laurila, A., Loyau, A., Martel, A., Meurling, S., Miad, C., Minting, P., Pasmans, F., Schmeller, D.S., Schmidt, B., R., Shelton, J.M.G., Skerratt, L.F., Smith, F., Soto-Azat, C., Spagnoletti, M., Tessa, G., Toledo, L.F., Valenzuela-Sánchez, A., Verster, R., Vörös, J., Webb, R.J., Wierzbicki, C., Wombwell, E., Zamudio, K.R., Aanensen, D.M., James, T.Y., Thomas, M., Weldon, C., Bosch, J., Balloux, F., Garner, T.W.J., Fisher, M.C., 2018. Recent Asian origin of chytrid fungi causing global amphibian declines. *Science* 360, 621–627. <https://doi.org/10.1126/science.aar1965>.
- Orchard, S.A., 2011. Removal of the American bullfrog *Rana (Lithobates) catesbeiana* from a pond on a lake on Vancouver Island, British Columbia, Canada. *Int. Conf. Isl. Invasives* 217–221.
- Othman, S.N., Chen, Y.-H., Chuang, M.-F., Andersen, D., Jang, Y., Borzée, A., 2020a. Impact of the mid-pleistocene revolution and anthropogenic factors on the dispersion of Asian Black-spined toads (*Duttaphrynus melanostictus*). *Animals* 10, 1157. <https://doi.org/10.3390/ani10071157>.
- Othman, S.N., Chuang, M.F., Kang, H., Bae, Y., Kim, A., Jang, Y., Borzée, A., 2020b. Methodological guidelines for minimally invasive tail-clipping: a case study on *Rana huanrenensis* tadpoles. *Asian J. Conserv. Biol.* 9, 188–195.
- Park, J., Grajal-Puche, A., Roh, N.H., Park, I.K., Ra, N.Y., Park, D., 2021. First detection of ranavirus in a wild population of Dybowsky's brown frog (*Rana dybowskii*) in South Korea. *J. Ecol. Environ.* 45, 2. <https://doi.org/10.1186/s41610-020-00179-2>.
- Puckridge, M., Andreakis, N., Appleyard, S.A., Ward, R.D., 2013. Cryptic diversity in flathead fishes (Scorpaeniformes: Platycephalidae) across the Indo-West Pacific uncovered by DNA barcoding. *Mol. Ecol. Resour.* 13, 32–42. <https://doi.org/10.1111/1755-0998.12022>.
- Puillandre, N., Lambert, A., Brouillet, S., Achaz, G., 2012. ABGD, Automatic Barcode Gap Discovery for primary species delimitation. *Mol. Ecol.* 21, 1864–1877. <https://doi.org/10.1111/j.1365-294X.2011.05239.x>.
- Pyšek, P., Jarošík, V., Hulme, P.E., Kühn, I., Wild, J., Arvanitou, M., Bacher, S., Chiron, F., Didžiulis, V., Essl, F., Genovesi, P., Gherardi, F., Hejda, M., Kark, S., Lambdon, P.W., Desprez-Loustau, M.L., Nentwig, W., Pergl, J., Poboljsaj, K., Rabitsch, W., Roques, A., Roy, D.B., Shirley, S., Solarz, W., Vilà, M., Winter, M., 2010. Disentangling the role of environmental and human pressures on biological invasions across Europe. *Proceedings of the National Academy of Sciences of the United States of America* 107, 12157–12162. <https://doi.org/10.1073/pnas.1002314107>.
- R Core Team, 2020. R: A language and environment for statistical computing. R Foundation for Statistical Computing, Vienna, Austria.
- Rambaut, A., Drummond, A.J., Xie, D., Baele, G., Suchard, M.A., 2018. Posterior summarization in Bayesian phylogenetics using Tracer 1.7. *Syst. Biol.* 67, 901–904. <https://doi.org/10.1093/sysbio/syy032>.
- Regehr, E.V., Wilson, R.R., Rode, K.D., Runge, M.C., Stern, H.L., 2017. Harvesting wildlife affected by climate change: a modelling and management approach for polar bears. *J. Appl. Ecol.* 54, 1534–1543. <https://doi.org/10.1111/1365-2664.12864>.
- Reid, N.M., Carstens, B.C., 2012. Phylogenetic estimation error can decrease the accuracy of species delimitation: A Bayesian implementation of the general mixed Yule-coalescent model. *BMC Evolut. Biol.* 12, 196. <https://doi.org/10.1186/1471-2148-12-196>.
- Revell, L.J., 2012. phytools: An R package for phylogenetic comparative biology (and other things). *Methods Ecol. Evol.* 3, 217–223. <https://doi.org/10.1111/j.2041-210X.2011.00169.x>.
- Robertson, J.M., Langin, K.M., Sillett, T.S., Morrison, S.A., Ghalambor, C.K., Funk, W.C., 2014. Identifying evolutionarily significant units and prioritizing populations for management on islands. *Monogr. West. North Am. Nat.* 7, 397–411. <https://doi.org/10.3398/042.007.0130>.
- Rosenberg, N.A., Pritchard, J.K., Weber, J.L., Cann, H.M., Kidd, K.K., Zhivotovsky, L.A., Feldman, M.W., We, 2002. Noah A. Rosenberg,^{1*} Jonathan K. Pritchard,² James L. Weber,³ Howard M. Cann,⁴ Kenneth K. Kidd,⁵ Lev A. Zhivotovsky,⁶ Marcus W. Feldman⁷ We. *Science* 298, 2381–2385.
- Rubinoff, D., Holland, B.S., 2005. Between two extremes: mitochondrial DNA is neither the panacea nor the nemesis of phylogenetic and taxonomic inference. *Syst. Biol.* 54, 952–961. <https://doi.org/10.1080/10635150500234674>.
- Sakai, A.K., Allendorf, F.W., Holt, J.S., Lodge, D.M., Molofsky, J., Orth, K.A., Baughman, S., Cabin, R.J., Cohen, J.E., Ellstrand, N.C., McCauley, D.E., O'Neil, P., Parker, I.M., Thompson, J.N., Weller, S.G., 2001. The population biology of invasive species. *Annu. Rev. Ecol. Syst.* 32, 305–332. <https://doi.org/10.1146/annurev.ecolsys.32.081501.114037>.
- Savage, J.M., 1975. Systematics and distribution of the Mexican and Central American stream frogs related to *Eleutherodactylus rugulosus*. *Copeia* 254. <https://doi.org/10.2307/1442883>.
- Schloegel, L.M., Picco, A.M., Kilpatrick, A.M., Davies, A.J., Hyatt, A.D., Daszak, P., 2009. Magnitude of the US trade in amphibians and presence of *Batrachochytrium dendrobatidis* and ranavirus infection in imported North American bullfrogs (*Rana catesbeiana*). *Biol. Conserv.* 142, 1420–1426. <https://doi.org/10.1016/j.biocon.2009.02.007>.
- Shin, Y., Jang, Y., Allain, S.J.R., Borzée, A., 2020. Catalogue of herpetological specimens of the Ewha Womans University Natural History Museum (EWNHM), Republic of Korea. *ZooKeys* 965, 103–139. <https://doi.org/10.3897/zookeys.965.52976>.
- Shine, R., Amiel, J., Munn, A.J., Stewart, M., Vyssotski, A.L., Lesku, J.A., 2015. Is “cooling then freezing” a humane way to kill amphibians and reptiles? *Biol. Open* 4, 760–763. <https://doi.org/10.1242/bio.012179>.
- Song, J.Y., Matsui, M., Chung, K.H., Oh, H.S., Zhao, W., 2006. Distinct specific status of the Korean brown frog, *Rana amurensis coreana* (Amphibia: Ranidae). *Zool. Sci.* 23, 219–224. <https://doi.org/10.2108/zsj.23.219>.
- Stouthamer, R., Nunney, L., 2014. Can neutral molecular markers be used to determine the success of an introduction of a “better” strain into an established population of a biocontrol parasitoid? *J. Econ. Entomol.* 107, 483–495. <https://doi.org/10.1603/ec13444>.
- Talavera, G., Dincă, V., Vila, R., 2013. Factors affecting species delimitations with the GMYC model: Insights from a butterfly survey. *Methods Ecol. Evol.* 4, 1101–1110. <https://doi.org/10.1111/2041-210X.12107>.
- Tamura, K., Stecher, G., Peterson, D., Filipski, A., Kumar, S., 2013. MEGA6: molecular evolutionary genetics analysis version 6.0. *Mol. Biol. Evol.* 30, 2725–2729. <https://doi.org/10.1093/molbev/mst197>.
- Taylor, B.L., Archer, F.I., Martien, K.K., Rosel, P.E., Hancock-Hanser, B.L., Lang, A.R., Leslie, M.S., Mesnick, S.L., Morin, P.A., Pease, V.L., Perrin, W.F., Robertson, K.M., Parsons, K.M., Viricel, A., Vollmer, N.L., Cipriano, F., Reeves, R.R., Krützen, M., Baker, C.S., 2017. Guidelines and quantitative standards to improve consistency in cetacean subspecies and species delimitation relying on molecular genetic data. *Mar. Mammal. Sci.* 33, 132–155. <https://doi.org/10.1111/mms.12411>.
- The Cochrane Collaboration, 2020. Review Manager (RevMan) [Computer program] Version 5.4.
- Vandome, C., Vines, A., 2018. Tackling illegal wildlife trade in Africa economic incentives and approaches. *R. Inst. Int. Aff.* 1–26.
- Vences, M., Thomas, M., Meijden, A., Van Der, Chiari, Y., Vieites, D.R., 2005. of Amphibians. *Front. Zool.* 12, 1–12. <https://doi.org/10.1186/1742-9994-2-5>.
- Vences, M., J. Susanne Hauswaldt, S.S., Rupp, O., Goessmann, A., Künzel, S., Pablo Orozco-terWengel, D.R.V., Nieto-Roman, S., Haas, S., Laugsch, C., Gehara, M., Bruchmann, S., Pabijan, M., Ludewig, A.K., Rudert, D., Angelini, C., Borkin, L.J., Pierre-Andre Crochet, A.C., Dubois, A., Ficetola, G.F., Galán, P., Geniez, P., Hachtel, M., Jovanovic, O., Litvinchuk, S.N., Lymerakis, P., Ohler, A., Smirnov, N.A., 2013. Radically different phylogeographies and patterns of genetic variation in two European brown frogs, genus *Rana*. *Mol. Phylogenetics Evol.* 68, 657–670. <https://doi.org/10.1093/jhered/esr136>.
- Waddle, J.H., Grear, D.A., Mosher, B.A., Grant, E.H.C., Adams, M.J., Backlin, A.R., Barichivich, W.J., Brand, A.B., Bucciarelli, G.M., Calhoun, D.L., Chestnut, T., Davenport, J.M., Dietrich, A.E., Fisher, R.N., Glorioso, B.M., Halstead, B.J., Espinal, J.A.L., Lorch, J.M., McCreary, B., Muths, E., Pearl, C.A., Richgels, K.L.D., Robinson, C.W., Roth, M.F., Rowe, J.C., Sadinski, W., Sigafus, B.H., Stasiak, I., Sweet, S., 2020. *Batrachochytrium salamandrivorans* (Bs) not detected in an intensive survey of wild North American amphibians. *Sci. Rep.* 10, 13012. <https://doi.org/10.1038/s41598-020-69486-x>.

- Yan, F., Lü, J., Zhang, B., Yuan, Z., Zhao, H., Huang, S., Wei, G., Mi, X., Zou, D., Xu, W., Chen, S., Wang, J., Xie, F., Wu, M., Xiao, H., Liang, Z., Jin, J., Wu, S., Xu, C.S., Tapley, B., Turvey, S.T., Papenfuss, T.J., Cunningham, A.A., Murphy, R.W., Zhang, Y., Che, J., 2018. The Chinese giant salamander exemplifies the hidden extinction of cryptic species. *Curr. Biol.* 28, R590–R592. <https://doi.org/10.1016/j.cub.2018.04.004>.
- Yang, B., Lu, Y., Li, P., 2010. Discussion on validity of *Rana maoershanensis* based on partial sequence of 16S rRNA gene. *Asian Herpetological Research* 1, 97–102. <https://doi.org/10.3724/SP.J.1245.2010.00097>.
- Yang, B.T., Zhou, Y., Min, M.S., Matsui, M., Dong, B.J., Li, P.P., Fong, J.J., 2017. Diversity and phylogeography of Northeast Asian brown frogs allied to *Rana dybowskii* (Anura, Ranidae). *Mol. Phylogenetics Evol.* 112, 148–157. <https://doi.org/10.1016/j.ympev.2017.04.026>.
- Yang, L., Tan, Z., Wang, D., Xue, L., Guan, M.X., Huang, T., Li, R., 2014. Species identification through mitochondrial rRNA genetic analysis. *Sci. Rep.* 4, 1–11. <https://doi.org/10.1038/srep04089>.
- Yu, G., Rao, D., Matsui, M., Yang, J., 2017. Coalescent-based delimitation outperforms distance-based methods for delineating less divergent species: the case of *Kurixalus odontotarsus* species group. *Sci. Rep.* 7, 16124. <https://doi.org/10.1038/s41598-017-16309-1>.
- Yuan, Z.Y., Zhou, W.W., Chen, X., Poyarkov, N.A., Chen, H.M., Jang-Liaw, N.H., Chou, W.H., Matzke, N.J., Iizuka, K., Min, M.S., Kuzmin, S.L., Zhang, Y.P., Cannatella, D.C., Hillis, D.M., Che, J., 2016. Spatiotemporal diversification of the true frogs (Genus *Rana*): a historical framework for a widely studied group of model organisms. *Syst. Biol.* 65, 824–842. <https://doi.org/10.1093/sysbio/syw055>.
- Zhang, J., Kapli, P., Pavlidis, P., Stamatakis, A., 2013. A general species delimitation method with applications to phylogenetic placements. *Bioinformatics* 29, 2869–2876. <https://doi.org/10.1093/bioinformatics/btt499>.
- Zhao, Y., Yi, Z., Warren, A., Song, W.B., 2018. Species delimitation for the molecular taxonomy and ecology of the widely distributed microbial eukaryote genus *Euplotes* (Alveolata, Ciliophora). *Proc. R. Soc. B: Biol. Sci.* 285, 20172159. <https://doi.org/10.1098/rspb.2017.2159>.
- Zhou, W.-W., Wen, Y., Fu, J., Xu, Y.B., Jin, J.Q., Ding, L., Min, M.S., Che, J., Zhang, Y.P., 2012. Speciation in the *Rana chensinensis* species complex and its relationship to the uplift of the Qinghai-Tibetan Plateau. *Mol. Ecol.* 21, 960–973. <https://doi.org/10.1111/j.1365-294X.2011.05411.x>.
- Zhou, Y., Yang, B.-T., Li, P.-P., Min, M.-S., Fong, J.J., Dong, B.-J., Zhou, Z.-Y., Lu, Y.-Y., 2015. Molecular and morphological evidence for *rana kunyuensis* as a junior synonym of *rana coreana* (Anura: Ranidae). *J. Herpetol.* 49, 302–307. <https://doi.org/10.1670/13-111>.